CANADIAN JOURNAL OF RESEARCH

VOLUME 16 JULY, 1938 NUMBER 7

CONTENTS

SEC. A—PHYSICAL SCIENCES

SEC. B.—CHEMICAL SCIENCES

NATIONAL RESEARCH COUNCIL
OTTAWA, CANADA

Publications and Subscriptions

The Canadian Journal of Research is issued monthly in four sections, as follows:

A. Physical Sciences
B. Chemical Sciences
C. Botanical Sciences
D. Zoological Sciences

For the present, Sections A and B are issued under a single cover, as also are Sections C and D, with separate pagination of the four sections, to permit separate binding, if desired.

Subscription rates, postage paid to any part of the world, are as follows:

	Annual	*Single Copy*
A and B	$ 2.50	$ 0.25
C and D	2.50	0.25
Four sections, complete	4.00	—

The Canadian Journal of Research is published by the National Research Council of Canada under the authority of the Chairman of the Committee of the Privy Council on Scientific and Industrial Research. All correspondence should be addressed:

National Research Council, Ottawa, Canada.

Canadian Journal of Research

Issued by THE NATIONAL RESEARCH COUNCIL OF CANADA

VOL. 16, SEC. A. JULY, 1938 NUMBER 7

THE REFRACTIVE INDICES OF LIQUID HELIUM I AND HELIUM II[1]

BY H. E. JOHNS[2] AND J. O. WILHELM[3]

Abstract

The refractive indices of liquid Helium I and Helium II were measured by means of a Wollaston cell. The value obtained with λ5461 Å for He I at 4.2° K was 1.0206 ± 0.0012; for He I at 2.26° K, 1.0269 ± 0.0004; and for He II at 2.18° K, 1.0269 ± 0.0004. It was also shown that the index changed by less than ±0.00007 in passing from a point in He I to a point with the same density in He II. It was concluded, therefore, that there is no change in the molecular refractivity in passing from He I to He II.

Experimental

The apparatus employed was essentially the same as that used in the measurement of the refractive indices of liquid oxygen, nitrogen, and hydrogen, as described by the authors (1). In order to measure the very much smaller refractive index of liquid helium the optical arrangement was altered. Two vertical slits were used as a collimator; consequently, the light reached the cell in a very narrow parallel beam. When the cell was turned to large critical angles of approximately 80° it was found that the beam was deviated slightly. This was due to the fact that the cell was slightly prismatic at the edges and at such large angles, even with a narrow parallel beam, much of the light passed through the cell near its periphery. Because the rays were deviated, the telescope could not be used in a fixed position but had to be rotated to follow the image as the cell was turned. When the illumination suddenly disappeared the readings on the divided head were taken. Four settings were made in this manner, both sides of the cell being used. On account of the slight prismatic effect, readings on opposite sides of the cell did not differ by 180°, but the average of readings on opposite sides must give the correct critical angle very closely, unless the plates are badly distorted. Measurements made in this way with a telescope gave an estimated accuracy of 5′ in the critical angle, which corresponds to a variation of ±0.0004 in the index. The measurements in He I at 4.22° K. were considerably more difficult to make owing to the larger critical angle and the vigorous boiling which took place. Since there is less interest in the refractive index in this case, the eye alone was used to determine the position at which the light was cut off,

[1] *Manuscript received June 10, 1938.*
Contribution from the Department of Physics, University of Toronto, Toronto, Canada.

[2] *Holder of a bursary under the National Research Council of Canada.*

[3] *Assistant Professor, Department of Physics, University of Toronto, Toronto, Canada.*

and the setting was made only to the nearest tenth of a degree. With this method the critical angle was determined to within 20′ and the index to within ± 0.0012.

Results

The results obtained for λ 5461A° are given in Table I.

TABLE I

—	Temp., °K.	Critical angle	Refractive index	Density (2, 3)	$\frac{1}{\rho}\frac{\mu^2-1}{\mu^2+2}$
He I	4.22	78° 28′ ± 20′	1.0206 ± 0.0012	0.1255	0.109
He I	2.26	76° 51′ ± 5′	1.0269 ± 0.0004	0.1470	0.122
He II	2.18	76° 51′ ± 5′	1.0269 ± 0.0004	0.1470	0.122

In addition to making the above measurements, an effort was made to ascertain whether there was any measurable difference in the refractive indices of He I and He II at temperatures at which the liquids had the same density. For this purpose the telescope was set so that the last fringe of the interference pattern was placed in the middle of the image of the slit. Any very slight further turning of the cell would cause this last fringe to pass out of sight altogether, and thus the cell could be accurately set at the critical position. This was done with He II boiling under a pressure of 35 mm., corresponding to a temperature of 2.18° K, then the pressure was raised to 46 mm., corresponding to a temperature of 2.26° K, for which the helium had the same density. In this case the question of distortion by the plates of the cell does not enter and a change of 1′ could have been detected. The λ point was passed through several times in this way and no change in the position of the critical ray was observed. Therefore it is possible to state that the index changes by less than ± 0.00007 in passing from a point in He II to a point in He I which has the same density. We conclude, therefore, that He I and He II have the same molar refractivities.

The values obtained for the refractive indices agree with the preliminary value 1.028 ± 0.006 obtained by Wilhelm and Cove (4), as the index for He II. The refractive index was measured for one wave-length only, but the dispersion of liquid helium is plainly very small. The value of μ^2 at 2.18 ° K. is 1.0545, which corresponds closely to the dielectric constant, $K = 1.0558$ (5).

References

1. Johns, H. E. and Wilhelm, J. O. Can. J. Research, A, 15 : 101-108. 1937.
2. Mathias, E., Crommelin, C. A. and Onnes, H. K. Leiden Comm. 172b. 1925.
3. Onnes, H. K. and Boks, J. D. A. Leiden Comm. 170b. 1924.
4. Satterly, J. Rev. Modern Phys. 8 : 347-357. 1936.
5. Wolfke, M. and Keesom, W. H. Leiden Comm. 192a. 1927

A NEW FORM OF GAS THERMOMETER FOR USE AT VERY LOW TEMPERATURES[1]

By A. H. Woodcock[2]

Abstract

A new form of helium gas thermometer is described, which is designed for permanent installation in low temperature equipment in order to cover the difficult region between the temperatures of liquid hydrogen and of liquid helium. The device departs radically from the usual gas thermometer practice by having the volume of gas which remains at room temperature considerably larger than that of the thermometer bulb proper. It is shown theoretically that by this means the sensitivity, as compared with that of an ordinary gas thermometer with the same initial pressure and temperature, is greatly increased at the lowest temperatures. Thus it is possible to construct a thermometer which is sufficiently sensitive in the region below 20° K. to read temperatures to within 0.1° with the aid of an ordinary mercury manometer, and yet have a pressure only of the order of one atmosphere at room temperature. An experimental test has shown that the device is entirely practicable.

Introduction

The choice of suitable working thermometers for temperatures attainable with the aid of liquid hydrogen and liquid helium is a matter of some difficulty in practical low temperature work, and it is necessary to use different types of thermometer for different temperature ranges. From room temperature down to the boiling point of liquid hydrogen, 20° K, resistance thermometers are extensively used, being accurate, sensitive, and convenient. Between 20 and 14° K the vapor pressure of the hydrogen in the cryostat gives an entirely satisfactory measure of the temperature, and between 4.2 and 1.5° K the vapor pressure of helium is similarly used. The greatest difficulty arises in the range between 14 and 4° K. In this range the electrical thermometers become much less sensitive, requiring elaborate methods for the measurement of the small changes of resistance or thermal e.m.f., and it is frequently simpler to use a helium gas thermometer.

In the usual types of gas thermometer, care is taken to make the volume of gas in the connecting tubes leading to the manometer, the "dead space" which remains at room temperature, as small as possible. If it is desired to make a thermometer of this type a permanent part of the low temperature equipment, it would probably be filled to a pressure of the order of one atmosphere at room temperature. Its sensitivity is then inconveniently small for measurements of reasonable accuracy in the range desired. Sufficient sensitivity can be obtained by making the pressure approximately atmospheric at the hydrogen point, but this involves either refilling the thermometer every time it is used, or making the construction heavy enough to withstand a large pressure at room temperature.

The thermometer to be described in the present paper is designed to be sufficiently sensitive in the range from 14 to 4° K to make readings to within

[1] *Manuscript received June 10, 1938.*
Contribution from the Department of Physics, University of Toronto, Toronto, Canada.

[2] *At the time, Demonstrator, Department of Physics, University of Toronto.*

0.1° with ease, and yet to have a sufficiently small pressure at room temperature that the thermometer can be permanently installed in a helium liquefier. This end is achieved by departing radically from the usual practice in the construction of gas thermometers, and making the volume of gas which remains at room temperature considerably larger than that of the thermometer bulb proper (see Fig. 1). It is still advisable to make the volume of the connecting tube, along which there is a temperature gradient, as small as is compatible with reasonably rapid action.

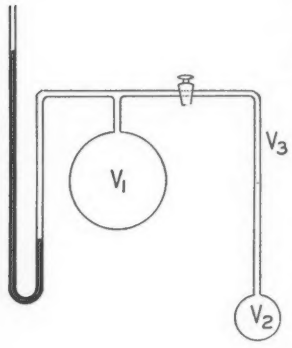

FIG. 1. *Double bulb gas thermometer.*

Although the field of usefulness of this type of thermometer is rather limited, the proposal aroused such argument that the author thought it would be of interest to construct one and test it, and that the possibility of its use might be of interest to others.

In appearance the construction is somewhat similar to the gas thermometer recently described by Mendelssohn and Pontius (1). However, the two devices are fundamentally different in their action, and in the function of the upper bulb. The thermometer designed by Mendelssohn and Pontius is intended for the measurement of small temperature changes, and, like an ordinary helium thermometer which has atmospheric pressure at liquid hydrogen temperature, has to be refilled every time it is used.

Theory

In considering the theoretical behavior of the thermometer in question, certain simplifying assumptions can be made, since it is not intended to be used when extreme accuracy is required. It will be assumed:

1. That the gas used can be treated as a perfect gas throughout the range. This will be very nearly true for pure helium from 14 to 4° K, since the pressure at the lower end of the range is considerably less than atmospheric.

2. That a steady state is reached in a reasonably short time, after which the gas in any part of the thermometer and connections is at the same temperature as the immediate surroundings in the cryostat equipment, and effects due to any further exchange of gas between the two bulbs can be neglected.

3. That thermomolecular pressure differences can be neglected in comparison with the pressures to be measured.

4. That changes in volume of the bulbs can be neglected.

Consider first a gas thermometer of the usual type, in which all volumes are negligible except that of the lower bulb. Let it be filled at room temperature

T_1 to a pressure π_1. Then at the low temperature T the pressure is given by

$$\pi = \pi_1 T/T_1 \tag{1}$$

and the sensitivity by

$$d\pi/dT = \pi_1/T_1 \tag{2}$$

which is constant over the whole temperature range.

Next consider a thermometer of the type shown in Fig. 1, in which a volume V_1 is kept at a temperature T_1, and only the volume V_2 is subjected to the low temperature T which it is required to measure. When the thermometer is first filled we have volume $V_1 + V_2$, all at pressure and temperature P_1, T_1. When it is in use we have a volume V_1 at pressure and temperature P, T_1, and a volume V_2 at the same pressure P but temperature T. Since the total mass of gas is constant.

$$P_1V_1/T_1 + P_1V_2/T_1 = PV_1/T_1 + PV_2/T$$

or

$$P = \frac{P_1T(V_1 + V_2)}{(V_1T + V_2T_1)} = \frac{P_1T}{T_1} \frac{1 + v}{1 + vT/T_1}, \tag{3}$$

where $v = V_1/V_2$ is the volume ratio.

Then the sensitivity is given by

$$\left(\frac{\partial P}{\partial T}\right)_{T_1 \text{ constant}} = \frac{P_1}{T_1} \frac{1 + v}{(1 + vT/T_1)^2} \tag{4}$$

When T/T_1 is small this sensitivity becomes considerably greater than the sensitivity (Equation (2)) of an ordinary gas thermometer, supposing the initial pressure and temperature to be the same. It follows also from Equation (4) that, while an increase in the volume ratio v will increase the sensitivity at very low temperatures, it will decrease the range of temperature over which the gain in sensitivity occurs.

In operation, the upper bulb V_1 is supposed to be kept at a constant temperature T_1, and it is necessary to investigate the errors due to fluctuations in this temperature. Let the temperature of V_1 change to T_1', and the measured pressure to P', while the lower temperature remains equal to T. We now have

$$P_1V_1/T_1 + P_1V_2/T_1 = PV_1/T_1 + PV_2/T = P'V_1/T_1' + P'V_2/T,$$

which gives

$$P' = \frac{P_1T}{T_1} \frac{1 + v}{1 + vT/T_1'},$$

and

$$\left(\frac{\partial P'}{\partial T_1'}\right)_{T \text{ constant}} = \frac{P_1}{T_1} \frac{T^2}{T_1'^2} \frac{v(1 + v)}{(1 + vT/T_1')^2}$$

If T_1' is approximately equal to T_1, *i.e.*, $(T_1 - T_1')$ small compared with $(T_1 - T)$, this reduces to

$$\left(\frac{\partial P'}{\partial T_1'}\right)_T = v\left(\frac{T}{T_1}\right)^2\left(\frac{\partial P}{\partial T}\right)_{T_1} \tag{5}$$

Therefore, when T is small, changes in temperature of the upper bulb have a very much smaller effect upon the pressure than changes in the temperature to be measured.

The effect of the finite volume of the connecting tube can be taken into account by considering an additional small volume V_3 at a temperature T_3, intermediate between T and T_1. An expression for the correction can easily be obtained if it can be assumed that the temperature gradient is uniform along the tube. However, this assumption may be far from correct in practice, and it is likely to be more satisfactory to take account of this, and other small errors, by calibrating the thermometer at two or three known temperatures, under actual working conditions.

Table I shows, for a thermometer with a volume ratio $V_1/V_2 = 10$, filled to a pressure of 100 cm. of mercury at 300° K, the calculated sensitivity at different temperatures, the calculated fluctuation due to changes in the temperature of the upper bulb, and the sensitivity as compared with an ordinary gas thermometer under the same initial conditions.

TABLE I

$V_1 = 10V_2$, $P_1 = 100$ cm., $T_1 = 300°$ K

T °K	$\left(\frac{\partial P}{\partial T}\right)_{T_1}$ cm./°K	$\left(\frac{\partial P}{\partial T_1}\right)_{T}$ cm./°K	Sensitivity as compared with ordinary thermometer
300	0.030	0.303	0.09
200	0.062	0.277	0.19
100	0.195	0.217	0.64
50	0.515	0.143	1.7
20	1.32	0.059	4.4
15	1.63	0.041	5.4
10	2.06	0.023	6.8
5	2.69	0.008	8.9

It will be seen that when the lower bulb is at 15° K, a change of 4° in the temperature of the upper bulb has the same effect as a change of only 0.1° in the temperature to be measured. For accurate work the upper bulb ought to be kept in ice, or in a water bath at a known temperature, but for many purposes this refinement could be neglected.

Experimental Test

As a check on the calculations, a thermometer was made up as shown in Fig. 1, with volumes $V_1 = 320$ cc., $V_2 = 39.7$ cc., and V_3 about 6 cc. It was filled with pure helium to a pressure of 76.7 cm. at a temperature of 22.5° C. The gas was used first to determine the volume of the manometer connections, which form a part of the volume V_1. This was accomplished by shutting off V_2 with a tap, and then noting the change in pressure when V_1 was immersed in liquid air.

With the initial conditions stated above, the pressure to be expected at the boiling point of liquid hydrogen, 20.45° K, was calculated by Formula (3), and found to be 31.16 cm. The measured pressure with the bulb V_2 in hydrogen boiling at atmospheric pressure, and V_1 simply exposed to the room, was 30.7 cm.

The curve in Fig. 2 shows the calculated relation between pressure and the temperature T of the lower bulb, for the thermometer used. The dotted

straight line shows the behavior of an ordinary gas thermometer, with V_1 negligible, under the same initial conditions. The circle marks the test reading made at hydrogen temperature. The agreement is close enough to show that the predicted gain in sensitivity is actually attained at temperatures below about 80° K, and that the device is entirely practicable. It ought, however, to be calibrated at two or three known temperatures, under actual working conditions, in order to allow for small errors due to the connecting tube, and other causes.

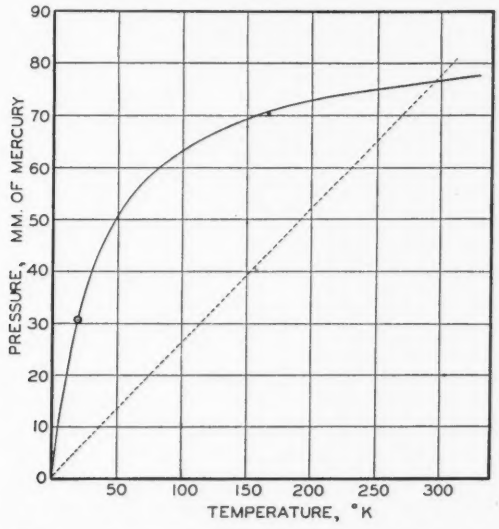

FIG. 2. *Theoretical curve for double bulb gas thermometer.*

Acknowledgments

The author wishes to express his thanks to Prof. E. F. Burton for his encouragement and interest, and to Prof. J. Satterly and Prof. H. Grayson Smith for many helpful discussions.

Reference

1. MENDELSSOHN, K. and PONTIUS, R. B. Phil. Mag. 24 : 777-787. 1937.

VIBRATION OF POWER LINES IN A STEADY WIND

IV. NATURAL FREQUENCIES OF VIBRATION OF STRINGS WITH STRENGTHENED ENDS[1]

By R. Ruedy[2]

Abstract

When the mass of unit length of a string of length $2L$, instead of being uniform, increases from the centre toward the ends according to the law $(1 + x/L)^m$, the natural frequencies of vibration are lower than those of the uniform string, but the ratios between the frequencies of successive overtones remain virtually unchanged, and with the exception of the first one or two overtones agree with those of a uniform string having a mass per unit length $(2(1 + \lambda)^{(m+2)/2} - 1)/\lambda(m + 2)$ times that at the centre of the strengthened string. The reduction in the natural frequencies of vibration is, of course, larger the greater the ratio between the masses at the two ends, whereas the value of m has a relatively small influence. The overtones form two distinct series: one, corresponding to the harmonics of even order, is always present; the other, corresponding to the harmonics of odd order, is suppressed when the density of the string increases from one end to the other (unsymmetrical span).

Introduction

Various measures are taken in order to suppress, or at least reduce, the vibrations invariably present when steady winds blow against the span of a transmission line strongly stretched by its own weight. Since in the course of time the vibrations injure the conductor near the point at which the wires are fastened to the insulating supports, special clamps and holders have been designed to relieve the strain; but as little is known about the stresses that arise when a transverse wave is reflected at the end of a string, an unfailing remedy in the nature of an improved clamp has yet to be found (5). Other devices, the vibration dampers, are intended to reduce the amplitudes of vibration to less than about one-tenth of the amplitude observed along the unprotected span (3, 4). Dampers are attached to the power line, at one or several points within the same span; as they partake of the vibrations of the conductor, they absorb energy inherent in the motion of the wire and reduce the amplitudes of the displacements. The construction of the dampers varies from simple weights at one end or both ends of a flexible bar (so-called torsion damper and Stockbridge dumbbell) to shock absorbers with spring suspension and oil or air damping (Holt damper), and from simple loops or festoons of wire, loosely or firmly tied to the first and last feet of the span, to the design in which the conductor is separated into an external hollow conductor resting on a supporting core (Preiswerk line). In view of the requirements in regard to design, material, and adjustment necessitated by the use of vibration dampers, the simple expedient of strengthening the ends of the string by merely adding to its thickness is remarkably successful in comparison. Various methods of stiffening the conductor near the clamps and increasing its resistance

[1] *Manuscript received June 14, 1938.*

Contribution from the Division of Research Information, National Research Laboratories, Ottawa, Canada.

[2] *Research Investigator, National Research Laboratories, Ottawa.*

to bending forces are in practical use: in one method, sleeves, slightly tapered on the inner side, are screwed around the conductor on both sides of the clamp; in another method, pieces several feet long, of the conductor used, are tied to the ends, or are strung along the conductor, by means of auxiliary clamps, an arrangement known as armor rods, or a piece of strong wire is wound around the ends. Flexible blades of metal are sometimes added in place of rods.

On the 220 kv. line, 125 miles long, from Beauharnois over Cumberland and South March (Ontario) to the Chats Falls on the Ottawa, a line built in 1932, a helix of round rods is twisted around the conductor in order to dampen the vibrations near the end of the wire. Festoon dampers are used on the 55 mile stretch of the 110 kv. line built in 1934 for carrying Gatineau power from Ottawa to Cornwall.

Strengthening devices are simpler in their construction than vibration dampers, but when they have to be added to a line already completed it becomes necessary to untie the conductor at the clamp. They reduce the amplitudes of vibration near the ends only in proportion to their mass. The effects to be expected when the strengthening member forms a constituent part of the wire, and is subject to the same tension as the conductor, have not hitherto been examined. A study of this problem, the string with strengthened ends, is of interest not only as regards the question of lessening vibrations and their injurious effects, but also as adding to our knowledge of non-harmonic vibrations in a field that lies particularly close at hand, since it embraces the problem of the uniform string as merely one particular case.

Equation of the Vibrating String of Finite Length *L*.

When the mass of unit length of a vibrating string of length L stretched by a constant tension S is a function $m(x)$ of the distance x from the origin, the transverse displacements y obey the differential equation

$$\frac{\partial^2 y}{\partial t^2} = \frac{S}{m(x)} \frac{\partial^2 y}{\partial x^2} .$$

The assumption that the solution is given by

$$y = Y(x)T(t)$$

leads to the relation

$$T(t) = A_t \sin \omega t + B_t \cos \omega t$$

for the time function, and to the relation

$$\frac{d^2 Y}{dx^2} + \frac{\omega^2}{S} m(x) Y = 0$$

for the curve described by the vibrating string. Strings of very different lengths will have to be considered; consequently, it is advisable to express distances and displacements in fractions of the length L of the string. In order that the equation for Y remain valid in the new units of length, the

function expressing the mass per unit length has to be multiplied by L, and the force or tension S divided by L, since forces have the dimension MLT^{-2}. At the same time, a function $\rho(x/L)$ takes the place of $m(x)$. With

$$\eta = Y/L \quad \text{and} \quad \xi = x/L$$

the equation giving the curve described by the vibrating string becomes

$$\frac{d^2\eta}{d\xi^2} + \frac{\omega^2}{S} L^2\rho(\xi)\eta = 0 .$$

The string with constant density is readily included in the treatment if the mass of unit length of the string is assumed to obey the law

$$\rho(\xi) = \rho_0(1 + \lambda\xi)^m,$$

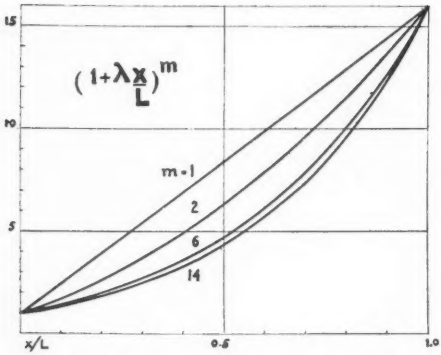

FIG. 1. *Density variations along the string for* $(1+\lambda)^m = 16$ *and various values of* m.

where m, as a general rule, is a whole number. The mass per unit length is equal to ρ_0 at that end of the string which is taken as the origin, and equal to $\rho_0(1 + \lambda)^m$ at the distant end of the string. When m is a large, and λ a small, number, the mass density increases gradually near the origin, and more and more abruptly as the other end is approached. In practice the mass of an element of a string or conductor that is strengthened at the end is at the farther end from 5 to 20 times as great as it is at the origin. Tables I and II and Fig. 1 show the rates at which the mass varies along the string for different values of m when $(1+\lambda)^m = 4$ (Table I), $(1+\lambda)^m = 16$ (Fig. 1), and $(1+\lambda)^m = 25$ (Table II).

On choosing, finally, under these conditions

$$\xi_1 = 1 + \lambda\xi$$

as the independent variable, the equation of the string changes to

$$\frac{d^2\eta}{d\xi_1^2} + \omega^2 \frac{L^2}{\lambda^2} \frac{\rho_0}{S} \xi_1^m \eta = 0 .$$

Its solution in Bessel functions of the order $1/(m + 2)$ is (2)

$$\eta = C_1\sqrt{\xi_1}J_{\frac{1}{m+2}}\left(\frac{2}{m+2}\,\omega\frac{L}{\lambda}\sqrt{\frac{\rho_0}{S}}\,\xi_1^{\frac{m+2}{2}}\right) + C_2\sqrt{\xi_1}J_{-\frac{1}{m+2}}\left(\frac{2}{m+2}\,\omega\frac{L}{\lambda}\sqrt{\frac{\rho_0}{S}}\,\xi_1^{\frac{m+2}{2}}\right),$$

TABLE I

VALUES CONNECTED WITH $(1 + \lambda)^m = 4$ FOR $m = 1, 2, 6,$ AND 14, AND VARIOUS VALUES OF $\xi_1 = (1 + \lambda\xi)$

	$(1+\lambda) = 4$ $\lambda = 3$			$(1+\lambda)^2 = 4$ $\lambda = 1$			$(1+\lambda)^6 = 4$ $\lambda = 0.26$			$(1+\lambda)^{14} = 4$ $\lambda = 0.1041$		
	$\xi_1^{1/2}$	$\xi_1^{(m+2)/2}$	ξ_1^m	$\xi_1^{1/2}$	$\xi_1^{(m+2)/2}$	ξ_1^m	$\xi_1^{1/2}$	$\xi_1^{(m+2)/2}$	ξ_1^m	$\xi_1^{1/2}$	$\xi_1^{(m+2)/2}$	ξ_1^m
$\xi = \frac{x}{L}$												
0	1.0			1.0			1.0			1.0		
0.1	1.14	1.48	1.3	1.049	1.21		1.013	1.108	1.166	1.005	1.086	1.156
0.2	1.27	2.02	1.6	1.095	1.44		1.023	1.225	1.355	1.010	1.179	1.334
0.3	1.38	2.62	1.9	1.140	1.69		1.038	1.350	1.562	1.016	1 279	1.537
0.4	1.48	3.24	2.2	1.183	1.96		1.051	1.486	1.811	1.021	1.386	1.769
0.5	1.58	3.94	2.5	1.224	2.25		1.063	1.631	2.082	1.026	1.501	2.035
0.6	1.67	4.65	2.8	1.265	2.56		1.075	1.786	2.386	1.031	1.624	2.337
0.7	1.76	5.45	3.1	1.304	2.89		1.087	1.950	2.727	1.036	1.756	2.678
0.8	1.84	6.22	3.4	1.342	3.24		1.099	2.130	3.108	1.041	1.897	3.070
0.9	1.92	7.07	3.7	1.378	3.61		1.111	2.319	3.531	1.046	2.046	3.500
1.0	2.0	8	4.0	1.414	4.0		1.123	2.520	4.001	1.051	2.208	4.000
γ	0.64			0.66			0.68			0.69		

The last complete line represents the values of $(1 + \lambda)^{1/2}$, $(1 + \lambda)^{(m+2)/2}$ *and* $(1 + \lambda)^m$, *which are frequently required. The expression* γ *is also listed for later use.*

TABLE II

VALUES CONNECTED WITH THE DENSITY FUNCTION $\xi_1 = (1 + \lambda\xi)^m$ FOR $(1 + \lambda)^m = 25$ AND $m = 1, 2, 6,$ AND 14

	$(1+\lambda) = 25$ $\lambda = 24$			$(1+\lambda)^2 = 25$ $\lambda = 4$			$(1+\lambda)^6 = 25$ $\lambda = 0.71$			$(1+\lambda)^{14} = 25$ $\lambda = 0.2585$		
	$\xi_1^{1/2}$	$\xi_1^{(m+2)/2}$	ξ_1^m	$\xi_1^{1/2}$	$\xi_1^{(m+2)/2}$	ξ_1^m	$\xi_1^{1/2}$	$\xi_1^{(m+2)/2}$	ξ_1^m	$\xi_1^{1/2}$	$\xi_1^{(m+2)/2}$	ξ_1^m
$\xi = \frac{x}{L}$												
0	1.0			1.0			1.0			1.0		
0.1	1.84	6.23	3.4	1.18	1.96		1.035	1.316	1.51	1.011	1.224	1.43
0.2	2.41	14	5.8	1.34	3.24		1.069	1.701	2.22	1.024	1.496	2.03
0.3	2.86	23.39	8.2	1.48	4.84		1.101	2.165	3.19	1.037	1.817	2.84
0.4	3.26	34.65	10.6	1.61	6.76		1.133	2.718	4.48	1.049	2.198	3.97
0.5	3.61	47.05	13	1.74	9.0		1.164	3.371	6.19	1.062	2.644	5.48
0.6	3.92	60.24	15.4	1.84	11.56		1.194	4.135	8.41	1.075	3.173	7.54
0.7	4.22	75.15	17.8	1.95	14.44		1.223	5.022	11.25	1.086	3.783	12.34
0.8	4.49	90.52	20.2	2.05	17.64		1.252	6.045	14.86	1.098	4.499	13.90
0.9	4.75	107.2	22.6	2.14	21.16		1.280	7.216	19.39	1.109	5.330	18.70
1.0	5.0	125.0	25	2.24	25		1.308	8.551	25	1.121	6.292	25.0
γ	0.29			0.33			0.376			0.39		

or a sum of such terms, since the principle of the superposition applies even to the string of variable density. The solutions are readily checked by differentiation. The two conditions that the displacements remain permanently zero at $\xi = 0$ and at $\xi = 1$ furnish two equations valid at the origin and at the end of the string, and elimination of C_1 and C_2 from these two relations gives for the natural frequencies of vibration of the string the equation

$$J_{\frac{1}{m+2}}\left(\frac{2}{m+2}\,\omega\frac{L}{\lambda}\sqrt{\frac{\rho_0}{S}}\right)J_{-\frac{1}{m+2}}\left(\frac{2}{m+2}\,\omega\frac{L}{\lambda}\sqrt{\frac{\rho_0}{S}}\,(1+\lambda)^{\frac{m+2}{2}}\right)$$
$$- J_{-\frac{1}{m+2}}\left(\frac{2}{m+2}\,\omega\frac{L}{\lambda}\sqrt{\frac{\rho_0}{S}}\right)J_{\frac{1}{m+2}}\left(\frac{2}{m+2}\,\omega\frac{L}{\lambda}\sqrt{\frac{\rho_0}{S}}\,(1+\lambda)^{\frac{m+2}{2}}\right) = 0\,,$$

or, with

$$z = \frac{2}{m+2}\,\omega\frac{L}{\lambda}\sqrt{\frac{\rho_0}{S}}$$

$$J_{\frac{1}{m+2}}(z)J_{-\frac{1}{m+2}}\left(z(1+\lambda)^{\frac{m+2}{2}}\right) - J_{-\frac{1}{m+2}}(z)J_{\frac{1}{m+2}}\left(z(1+\lambda)^{\frac{m+2}{2}}\right) = 0\,.$$

In view of the occurrence of various Bessel functions of any order between 0 and $\frac{1}{2}$, a survey of the field by experimental means alone, without at least a preliminary mathematical study, would lead to serious difficulties.

The Frequency Equation

When the mass of an element of the string taken at the distant end greatly exceeds the mass of an element of the same length taken at the origin, the density function $(1 + \lambda\xi)^m$ reduces to $\lambda\xi^m$. The equation for η is

$$\eta = C_1\sqrt{\lambda\xi}\,J_{\frac{1}{m+2}}\left(\frac{2}{m+2}\,\omega\frac{L}{\lambda}\sqrt{\frac{\rho_0}{S}}\,(\lambda\xi)^{\frac{m+2}{2}}\right).$$

The constant C_2 is equal to zero since at the origin the value of $J_{1/(m+2)}$ is zero, and that of $J_{-1/(m+2)}$ is infinity. The frequencies are determined by the solutions, j_n, of the Bessel function $J_{1/(m+2)}$

$$J_{\frac{1}{m+2}}\left(\frac{2}{m+2}\,\omega L\sqrt{\frac{\rho_0}{S}}\,\lambda^{\frac{m}{2}}\right) = 0\,.$$

Hence only those frequencies are allowed for which

$$\omega = \frac{m+2}{2\lambda^{\frac{m}{2}}}\sqrt{\frac{S}{\rho_0}}\,\frac{j_n}{L}\,,$$

with $j_n = 2.9, 6.03, 9.2 \ldots$ for $J_{\frac{1}{3}}$; or $j_n = 2.8, 5.91, \ldots$ for $J_{\frac{1}{4}}$, and the limits 2.404, 5.520, 8.654, . . . set by J_0, whereas the equation for the uniform string is

$$\omega = n\,\frac{\pi}{L}\sqrt{\frac{S}{\rho_0}}\,.$$

In other words, when λ is assumed to be very large, the natural frequencies of vibration of the string strengthened at the end are very much lower than the frequencies of the stretched string with uniform mass per unit length.

In the more general case, the linear density of the string does not vanish at the origin, and the natural frequencies of vibration are determined by more complicated equations, such as, for instance, for $(1 + \lambda)^m = 4$,

$$J_{\frac{1}{3}}(z)J_{-\frac{1}{3}}(8z) - J_{-\frac{1}{3}}(z)\,J_{\frac{1}{3}}(8z) = 0, \text{ for } m = 1$$

with the solutions $z_1 = 0.44$, $z_2 = 0.90$, $z_3 = 1.35$.

$$J_{\frac{1}{4}}(z)J_{-\frac{1}{4}}(4z) - J_{-\frac{1}{4}}(z)J_{\frac{1}{4}}(4z) = 0, \text{ for } m = 2$$

with the solutions $z_1 = 1.025$, $z_2 = 2.10$.

$$J_{\frac{1}{8}}(z)J_{-\frac{1}{8}}(2.52z) - J_{-\frac{1}{8}}(z)J_{\frac{1}{8}}(2.52z) = 0, \text{ for } m = 6.$$

$$J_{\frac{1}{16}}(z)J_{-\frac{1}{16}}(2.208z) - J_{-\frac{1}{16}}(z)J_{\frac{1}{16}}(2.208z) = 0, \text{ for } m = 14.$$

For values of z less than 10, the solutions are determined by using the tables for $J_{\frac{1}{3}}$ and $J_{\frac{1}{4}}$ (2). It is known that when z is greater than about 10,

$$J_\nu(z) = \sqrt{\frac{2}{\pi z}}\left(\zeta_\nu(z)\cos\psi_1 - \xi_\nu(z)\sin\psi_1\right)$$

$$J_{-\nu}(z) = \sqrt{\frac{2}{\pi z}}\left(\zeta_\nu(z)\cos\psi_{11} - \xi_\nu(z)\sin\psi_{11}\right),$$

where

$$\psi_1 = z - \frac{\pi}{4} - \nu\frac{\pi}{2}$$

$$\psi_{11} = z - \frac{\pi}{4} + \nu\frac{\pi}{2}$$

$$\zeta_{+\gamma}(z) = 1 - \frac{(4\gamma^2 - 1)(4\gamma^2 - 3^2)}{1\,.\,2(8z)^2} + \frac{(4\gamma^2 - 1)(4\gamma^2 - 3^2)(4\gamma^2 - 5^2)(4\gamma^2 - 7^2)}{1\,.\,2\,.\,3\,.\,4(8z)^4} \ldots + R_p$$

$$\xi_{+\gamma}(z) = \frac{4\gamma^2 - 1}{8z} - \frac{(4\gamma^2 - 1)(4\gamma^2 - 3^2)(4\gamma^2 - 5^2)}{1\,.\,2\,.\,3(8z)^3} + \ldots R_p\,.$$

With the aid of these formulas it may be shown that for values of z greater than 10, that is, for vibrations of frequencies normally produced by a steady wind blowing against a power line:

$$J_\nu(z)J_{-\nu}(z(1+\lambda)^{\frac{m+2}{2}}) - J_{-\nu}(z)J_\nu(z(1+\lambda)^{\frac{m+2}{2}}) = J_\nu(z_1)J_{-\nu}(z_2) - J_{-\nu}(z_1)J_\nu(z_2)$$

$$= \frac{2}{\pi}\sin\nu\pi\sqrt{\frac{1}{z_1 z_2}}\Big(\sin(z_1 - z_2)\Big(\zeta(z_1)\zeta(z_2) + \xi(z_1)\xi(z_2)\Big) - \cos(z_1 - z_2)\Big(\zeta(z_1)\xi(z_2) - \xi(z_1)\zeta(z_2)\Big)\Big)$$

This expression becomes equal to zero when

$$\tan z\,(1 - (1+\lambda)^{\frac{m+2}{2}}) = \frac{\zeta(z)\xi(z(1+\lambda)^{\frac{m+2}{2}}) - \xi(z)\zeta(z(1+\lambda)^{\frac{m+2}{2}})}{\zeta(z)\zeta(z(1+\lambda)^{\frac{m+2}{2}}) + \xi(z)\xi(z(1+\lambda)^{\frac{m+2}{2}})}$$

The practical value of this formula is enhanced by the fact that for the values of ν and m here concerned, the ζ's reduce to unity and the ξ's to the first term of the series; consequently, for all the overtones excepting the second and perhaps the third the frequencies are given with an accuracy sufficient for all practical purposes by

$$\tan z\left((1+\lambda)^{\frac{m+2}{2}}-1\right) = \xi\left(z(1+\lambda)^{\frac{m+2}{2}}\right) - \xi(z)$$

that is

$$\tan z\left((1+\lambda)^{\frac{m+2}{2}}-1\right) = \frac{4\nu^2-1}{8z}\left(\frac{1}{(1+\lambda)^{\frac{m+2}{2}}}-1\right)$$

or

$$z\tan z\left((1+\lambda)^{\frac{m+2}{2}}-1\right) = \frac{4\nu^2-1}{8}\,\frac{(1+\lambda)^{\frac{m+2}{2}}-1}{(1+\lambda)^{\frac{m+2}{2}}}$$

On writing

$$\left((1+\lambda)^{\frac{m+2}{2}}-1\right) z\tan z\left((1+\lambda)^{\frac{m+2}{2}}-1\right) = \frac{4\nu^2-1}{8}\,\frac{\left((1+\lambda)^{\frac{m+2}{2}}-1\right)^2}{(1+\lambda)^{\frac{m+2}{2}}}$$

it is seen that after solving

$$x\tan x = c$$

where the value of the constant c depends on λ, ν, and m, the natural frequencies of vibration higher than the second or third overtone are found from the formula

$$2\pi f_n = \omega_n = x_n\,\frac{m+2}{2L}\,\frac{\lambda}{(1+\lambda)^{\frac{m+2}{2}}-1}\sqrt{\frac{S}{\rho_0}},$$

while for a string with a constant density throughout the length

$$\omega_n = n\,\frac{\pi}{L}\sqrt{\frac{S}{\rho_0}}.$$

A comparison between the frequencies of the string with strengthened ends and those of the uniform string is readily made with the aid of Table III which lists the values of γx_n for the examples illustrated in Tables I and II, and Fig. 1. The lowest frequencies are computed from the solutions z of the original frequency equation, namely

$$\omega_n = \lambda z_n\,\frac{m+2}{2L}\sqrt{\frac{S}{\rho_0}}.$$

Fig. 2 represents the function $x\tan x$ used for the higher frequencies. In the range of the solutions of the equation $x\tan x = c$, from values of x near zero to very large values, it will, of course, be found that, as x increases, smaller and smaller values of $\tan x$ are sufficient to equal a given value c; in other words, the solutions x_n tend to lie closer to multiples of π. Hence the values of ω_n for the higher overtones follow at intervals that are only a fraction,

$$\gamma = \frac{m+2}{2}\,\frac{\lambda}{(1+\lambda)^{\frac{m+2}{2}}-1},$$

of the interval π known to separate the natural pulsations of the uniform string, and a string with the uniform mass $\gamma^{-\frac{1}{2}}$ has the same higher resonance frequencies as the string along which the mass changes, although the shape of the waves differ in the two instances. As is to be expected, the frequencies are considerably reduced when the ratio $(1 + \lambda)^m$ between the mass at the distant end and the mass at the origin is high, whereas the exponent m exerts a relatively slight influence; consequently, a concentration of the added mass at or near the origin produces almost the same reduction in the resonance frequencies and the same advantages as a gradual increase in density along the entire length.

TABLE III

RESONANCE FREQUENCIES OF THE STRENGTHENED STRING IN MULTIPLES OF $\sqrt{S/\rho_0}/L$
(EVEN-NUMBERED OVERTONES)

	$(1+\lambda)^m = 4$				$(1+\lambda)^m = 16$				$(1+\lambda)^m = 25$			
$m = 0$	3.14	6.28	9.43	12.57	3.14	6.28	9.43	12.57	3.14	6.28	9.43	12.57
1	1.90	4.05		8.10								
		4.08	6.08	8.10		2.44	3.54	4.64		2	2.93	3.81
2	2.04	4.20			1.20	2.52						
		4.16	6.30	8.38		2.59	3.83	5.07		2.20	3.24	4.25
6		4.31	6.45	8.60		2.80	4.17	5.55		2.37	3.52	4.67
14		4.34	6.49	8.65		2.85	4.26	5.67		2.52	3.75	4.98

Where two slightly different results are given for the same value of m, the upper line refers to the solution obtained from the equation valid at all frequencies, the lower line to the solution valid at higher and higher frequencies, beginning, as a comparison shows, with the first overtone.

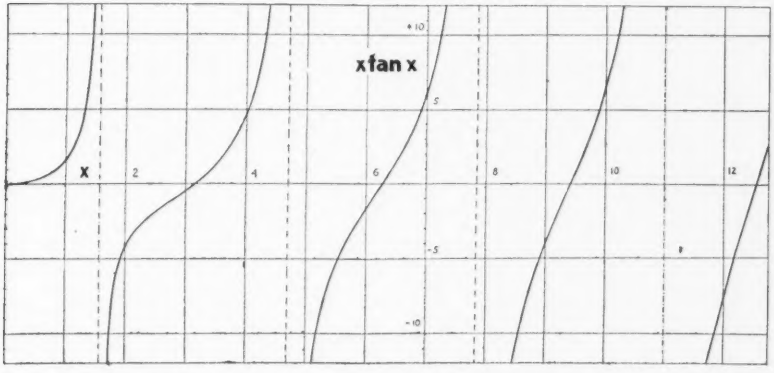

FIG. 2. *Values of x tan x for the determination of the overtones of the strengthened string with an even number of loops.*

Symmetrical String with Strengthened Ends

If a piece of wire is so attached to the string of length L that the density increases with the distance on the one as well as on the other side of the origin, while the centre is unconstrained, those natural frequencies of vibration which have a node at the centre and at the end, that is, the overtones with an even number of loops, remain unchanged and may simply be taken over from the unsymmetrical string. At the same time a new series of frequencies appears which show a loop at the centre of the span and nodes at both ends. If these boundary conditions are taken into account, the equation for the frequencies becomes

$$J_{\frac{m+1}{m+2}}\left(\frac{4}{m+2}\,\omega\,\frac{L}{\lambda}\sqrt{\frac{\rho_0}{S}}\right)J_{\frac{1}{m+2}}\left(\frac{4}{m+2}\,\omega\,\frac{L}{\lambda}\sqrt{\frac{\rho_0}{S}}\,(1+\lambda)^{\frac{m+2}{2}}\right)$$
$$+J_{-\frac{m+1}{m+2}}\left(\frac{4}{m+2}\,\omega\,\frac{L}{\lambda}\sqrt{\frac{\rho_0}{S}}\right)J_{-\frac{1}{m+2}}\left(\frac{4}{m+2}\,\omega\,\frac{L}{\lambda}\sqrt{\frac{\rho_0}{S}}\,(1+\lambda)^{\frac{m+2}{2}}\right)=0\,.$$

For instance, for $(1+\lambda)^m = 4$,

$$J_{\frac{2}{3}}(2z)J_{\frac{1}{3}}(16z)+J_{-\frac{2}{3}}(2z)J_{-\frac{1}{3}}(16z)=0,\quad\text{for}\quad m=1$$

with the approximate solutions $2z_1 = 0.26$; $2z_2 = 0.69\ldots$

$$J_{\frac{3}{4}}(2z)J_{\frac{1}{4}}(8z)+J_{-\frac{3}{4}}(2z)J_{-\frac{1}{4}}(8z)=0,\quad\text{for}\quad m=2$$

with the approximate solutions $2z_1 = 0.59$; $2z_2 = 1.6$

$$J_{\frac{7}{8}}(2z)J_{\frac{1}{8}}(5.04z)+J_{-\frac{7}{8}}(2z)J_{-\frac{1}{8}}(5.04z)=0,\quad\text{for}\quad m=6\,.$$

By using the series for large values of z it is easy to show that when as in the present example

$$\nu_2 = 1-\nu_1$$

then

$$J_{\nu_1}(z_1)J_{\nu_2}(z_2)+J_{-\nu_1}(z_1)J_{-\nu_2}(z_2)=$$
$$\sqrt{\frac{4}{\pi^2 z_1 z_2}}\cos(2\nu_1-1)\frac{\pi}{2}\Big(\cos(z_1-z_2)\Big(\zeta_{\nu_1}(z_1)\zeta_{\nu_2}(z_2)+\xi_{\nu_1}(z_1)\xi_{\nu_2}(z_2)\Big)$$
$$-\sin(z_1-z_2)\Big(\zeta_{\nu_1}(z_1)\xi_{\nu_2}(z_2)-\xi_{\nu_1}(z_1)\zeta_{\nu_2}(z_2)\Big)\Big)=0\,.$$

The roots larger than $z = 10$ are given by

$$\tan(z_1-z_2)=\frac{\zeta_{\nu_1}(z_1)\zeta_{\nu_2}(z_2)+\xi_{\nu_1}(z_1)\xi_{\nu_2}(z_2)}{\zeta_{\nu_1}(z_1)\xi_{\nu_2}(z_2)-\xi_{\nu_1}(z_1)\zeta_{\nu_2}(z_2)}\,.$$

For frequencies higher than that of the second or third overtone the expression reduces to

$$\tan z\left((1+\lambda)^{\frac{m+2}{2}}-1\right)=\cfrac{8z}{4\left(\frac{m+1}{m+2}\right)^2-1-\cfrac{4}{\frac{(m+2)^2}{(1+\lambda)^{\frac{m+2}{2}}}-1}}$$

an equation that can be written in the standard form

$$\frac{\tan x}{x}=c\,.$$

For instance, when $(1 + \lambda)^m = 4$, and where now $z = \frac{4}{m+2}\omega\frac{L}{\lambda}\sqrt{\frac{\rho_0}{S}}$,

$$\frac{\tan 7z}{7z} = 1.35 \text{ , for } m = 1, \text{ with the solutions } 7z = 0.87; 4.55; 7.76; 10.92$$

$$\frac{\tan 3z}{3z} = 1.855, \text{ for } m = 2, \text{ with the solutions } 3z = 1.12; 4.6; 7.785$$

$$\frac{\tan 1.52z}{1.52z} = 1.7 \text{ , for } m = 6$$

$$\frac{\tan 1.208z}{1.208z} = 2.24 \text{ , for } m = 14 .$$

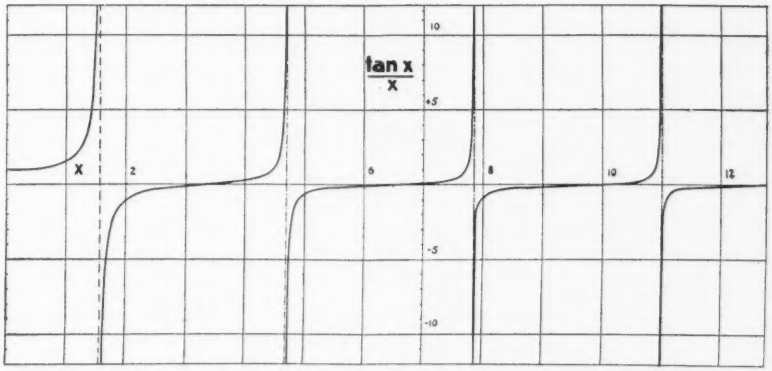

FIG. 3. *Values of tan x/x for the determination of the overtones of odd orders.*

It is known that when x lies between 0 and $\pi/2$ the ratio $\tan x/x$ is always larger than unity. As x begins to increase beyond the value π the ratio $\tan x/x$ increases from zero to very large values. The same growth is repeated each time that x has increased by the amount π, but, with each step, larger values of $\tan x$ are required in order to obtain a given ratio c (Fig. 3). In other words, at the higher frequencies the solutions x tend more and more toward the values $n\pi/2$. The higher overtones follow, therefore, from the equation

$$x_n = \left((1 + \lambda)^{\frac{m+2}{2}} - 1\right) z = \frac{4}{m+2}\left((1 + \lambda)^{\frac{m+2}{2}} - 1\right)\frac{\omega L}{\lambda}\sqrt{\frac{\rho_0}{S}}$$

or

$$\omega_n = x_n \frac{m+2}{4L}\frac{\lambda}{(1+\lambda)^{\frac{m+2}{2}} - 1}\sqrt{\frac{S}{\rho_0}} = \frac{\gamma}{2}\frac{x_n}{L}\sqrt{\frac{S}{\rho_0}} ,$$

whereas for the string of length $2L$ and constant mass ρ_0 per unit length

$$\omega_n = n\frac{\pi}{2L}\sqrt{\frac{S}{\rho_0}} .$$

When the solutions x_n lie sufficiently close to $n\pi/2$, the correction factor γ, as before, reduces the natural frequencies of the uniform string to the resonance frequencies of the string strengthened at the ends.

References

1. CARROLL, J. S. and KOONTZ, J. A. Elec. Eng. 55 : 490-493. 1936.
2. KARAS, K. Sitzber. Akad. Wiss. Wien, 145 : 797-826. 1936.
3. PIPES, L. A. Elec. Eng. 55 : 600-614. 1936.
4. RUEDY, R. Can. J. Research, 13A : 99-110. 1935.
5. STURM, R. G. Elec. Eng. 55 : 455-465; 673-388. 1936.

Canadian Journal of Research

Issued by THE NATIONAL RESEARCH COUNCIL OF CANADA

VOL. 16, SEC. B. JULY, 1938 NUMBER 7

A SOURCE OF MERCURY RESONANCE RADIATION OF HIGH INTENSITY FOR PHOTOCHEMICAL PURPOSES[1]

BY E. W. R. STEACIE[2] AND N. W. F. PHILLIPS[3]

Abstract

A lamp-reaction vessel system for photochemical purposes is described. This is very inexpensive and has an unusually high intensity of mercury resonance radiation (about 1.5×10^{-5} einsteins per sec.).

Introduction

A great deal of photochemical work is done by mercury photosensitization, and for this purpose a strong source of the resonance line at 2537 Å is essential. The ordinary mercury arc possesses many disadvantages. It runs hot, emits numerous lines other than the resonance lines, and the resonance lines themselves are partially reversed, even when the lamp is water cooled. On this account most recent photochemical work has been done with low pressure discharge lamps, a rare gas carrier being used. These require a starting potential of about 5000 v., but operate on 400 to 500 v. Such lamps are commercially available with very high intensities. In order to use the emitted light efficiently it is customary to employ an annular quartz reaction vessel with the lamp in the centre. Such a combination of lamp and reaction vessel is quite effective, but is very expensive. Furthermore, it lacks flexibility, since, on account of the expense, special lamps and reaction vessels cannot be designed for each investigation.

Description

To obviate the above disadvantages a lamp-reaction vessel system has been designed, which is very cheaply and easily made since only the actual emitting portion of the lamp is of quartz, the remainder being constructed of Pyrex glass. A sketch is given in Fig. 1.

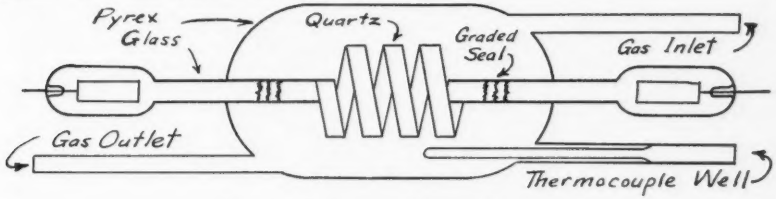

FIG. 1. *The lamp-reaction vessel system.*

[1] *Manuscript received May 2, 1938.*
Contribution from the Physical Chemistry Laboratory, McGill University, Montreal, with financial assistance from the National Research Council of Canada.

[2] *Associate Professor of Chemistry, McGill University.*
[3] *Demonstrator in Chemistry, McGill University.*

The emitting portion of the lamp is a quartz spiral constructed of tubing with an outside diameter of 10 mm. This is connected by graded seals to Pyrex tubing of the same diameter. The electrode chambers, also of Pyrex, are 15 mm. in diameter and 7 cm. long. The electrodes are standard neon sign "coated" electrodes, 8 mm. in diameter and 3 cm. long. They are welded through copper to tungsten wires which are sealed through the glass. The Pyrex reaction vessel is triple sealed on as shown, and is 9 cm. in diameter and 23 cm. long. The distance from the reaction vessel to the electrode chambers is 14 cm.

The lamp is filled with neon at a pressure of 12 mm., and contains a small droplet of mercury. The filling and "bombarding" of the electrodes was done by the usual neon sign technique* (1).

The coated electrodes were found to be very cool in operation, the electrode chambers being at a temperature not greater than 35° C. This is a considerable improvement on commercial lamps of this type with plain electrodes, which run at about 150° C. The smaller heating means improved efficiency. If it is desired to investigate reactions at high temperatures, either the central part of the lamp only may be heated, the electrodes being left outside the furnace, or, on account of the small heating of the electrodes, the entire lamp including the electrodes may be placed in the furnace.

The intensity of the resonance radiation emitted by the lamp was determined by measuring the rate of hydrolysis of monochloracetic acid (2). Two concentrations of the acid were employed, 0.5 *M* and 0.25 *M*. These gave identical results; absorption was therefore complete. The solution after irradiation was analyzed by the addition of an excess of silver nitrate and back titration, after filtration of the precipitated silver chloride, with potassium thiocyanate, ferric nitrate being used as an indicator. The characteristics of the lamp are given in Table I.

TABLE I

CHARACTERISTICS OF THE LAMP

Potential, v.	Current, ma.	Input, watts	Resonance radiation emitted, einsteins/sec.	Efficiency of production of λ 2537, %
450	120	54	1.62×10^{-5}	24
495	100	50	1.49	28
495	100	50	1.48	28
495	100	50	1.50	28
503	80	40	1.36	32
572	50	29	1.22	39
655	19	—	—	—
668	11	—	—	—
706	7.7	—	—	—
708	4.2	—	—	—
713	2.5	1.8	1.54×10^{-6}	80
820	1.9	—	—	—
920	1.7	—	—	—
1000	1.5	—	—	—
	<1.5	Lamp goes out		

* *We are greatly indebted to the Claude Neon Eastern Ltd., for performing these operations.*

The efficiency in Column 5 is calculated with allowance for the fact that one-half of the tubing is Pyrex glass and is opaque to λ 2537. As far as we are aware these are the highest efficiencies ever recorded for the production of λ 2537. The data at 100 ma. are illustrative of the constancy of the output. The lamp is remarkably stable at low currents, and can be operated efficiently without flickering down to 2.5 ma. Its intensity can thus be varied tenfold in operation.

References

1. MILLER, S. C. and FINK, D. G. Neon signs. McGraw-Hill Book Company, New York. 1935.
2. RUDBERG, E. Z. Physik, 24 : 247-263. 1924.

THE KINETICS OF THE DECOMPOSITION OF CHLOROPICRIN AT LOW PRESSURES[1]

By E. W. R. Steacie[2] and W. McF. Smith[3]

Abstract

The decomposition of gaseous chloropicrin has been investigated down to pressures of 0.3 cm. At lower pressures the rate falls off. The results fit the Kassel theory for a model with 15 oscillators, a molecular diameter of 8×10^{-8} cm., and a frequency of 779 cm.$^{-1}$

Introduction

A series of simple compounds differing only in the nature of their substituents, and decomposing at conveniently low temperatures, is of value in studying the effect of chemical constitution on the reaction rate. The series of which chloropicrin is a member constitutes such a group of compounds. In a previous paper (2) it was shown that the decomposition of chloropicrin is homogeneous and unimolecular, and consequently of value for comparative study. In view of this fact it was considered advisable to investigate the behavior of chloropicrin over a wider range of pressure, and this paper describes measurements carried out between 3.0 and 0.3 cm. initial pressure.

It was shown in the previous paper that the products of the decomposition are essentially nitrosyl chloride, phosgene, nitric oxide, and chlorine as represented stoichiometrically by the equations

$$CCl_3NO_2 \longrightarrow COCl_2 + NOCl$$
$$\updownarrow$$
$$NO + 1/2Cl_2.$$

There was evidence that the nitric oxide and chlorine are produced at a rate somewhat greater than that to be expected from the simple secondary decomposition of nitrosyl chloride.

Experimental

As in the previous work, the progress of the reaction was followed by observing the rate of pressure change in a system of constant volume. For experiments in which the initial chloropicrin pressure was greater than 1 cm. the apparatus was identical in design with that described in the preceding paper, except that mercury was replaced by butyl phthalate as a manometer liquid. As before, the pressure was measured with a glass manometer used as a null instrument, the reactant was introduced with the help of a magnetic hammer, and isolation of the system was accomplished by sealing off the connecting tubing. The dead space constituted about 5% of the reaction system.

In experiments in which the chloropicrin pressure was less than its vapor pressure at room temperature, *viz.*, about 1.5 cm., the reactant was admitted

[1] *Manuscript received June 8, 1938.*
Contribution from the Physical Chemistry Laboratory, McGill University, Montreal, Canada.

[2] *Associate Professor of Chemistry, McGill University.*
[3] *Holder of a studentship from the National Research Council of Canada.*

to the system and the system was isolated by a single stopcock greased with Apiezon N grease. The glass manometer employed in the investigation at pressures greater than 1.5 cm. was sensitive to better than 0.01 cm. of mercury, and that used for lower pressures was sensitive to 0.002 cm.

In this investigation the pressure increase at completion agreed with that to be expected from a mixture of phosgene, nitrosyl chloride, chlorine, and nitric oxide, with equilibrium established among the last three named. Thus at 161.7° C. and an initial pressure of 1.24 cm., the pressure increase at completion was 118% as compared with a calculated value of 119%.

For individual experiments the unimolecular constants calculated on the basis of the percentage pressure increase being equal to the amount of reaction show good agreement, rising somewhat with the progress of the reaction, particularly during the later stages as would be expected from the total pressure increase. On the other hand, the final equilibrium value is attained as quickly at low pressures as at high, and since the homogeneous decomposition of nitrosyl chloride is bimolecular, it would appear that nitric oxide and chlorine are produced in nearly the final equilibrium ratio during the initial decomposition, or that some surface catalyzed decomposition of nitrosyl chloride occurs. Rate constants calculated on the basis of nitric oxide and chlorine production in the final equilibrium amount show slightly better constancy than those calculated on the basis of percentage reaction corresponding to percentage pressure increase. However, the difference is small, and it has therefore been assumed that the time for a 25% pressure increase is a measure of the time for the same amount of decomposition to occur at different pressures. It is possible that on this basis a small error is introduced into the results, but in view of the semi-empirical nature of the theory of unimolecular reactions at low pressures such an error cannot be very serious.

TABLE I

COMPLETE DATA FOR TYPICAL EXPERIMENTS

Temperature, 161.7° C.

Initial pressure, 1.24 cm.			Initial pressure, 0.38 cm.		
Time, min.	Per cent reaction	$k \times 10^6$, sec.$^{-1}$	Time, min.	Per cent reaction	$k \times 10^6$, sec.$^{-1}$
5	6.8	235	6	6.7	192
10	13.6	243	12	13.5	194
15	20.9	261	18	19.2	197
20	27.4	267	24	24.7	196
25	35.3	240	30	30.2	197
30	39.6	280	36	36.5	210
35	45.5	289	42	41.0	202
40	50.0	281	49	46.1	210
51	59.5	295	55	51.5	201
60	65.5	296	60	55.8	226
80	79.0	325	71	60.0	213
100	88.0	354			

Results

Complete data for two runs are given in Table I. The rate constants given in this table are calculated on the assumption of equality between the percentage pressure increase and the amount of reaction. The summarized rate data for all runs are given in Table II. The high pressure values of t_{25} and t_{50} are given in Table III. These were obtained by plotting the corresponding values in Table II against the reciprocal of the initial pressure, and extrapolating to infinite pressure.

TABLE II

SUMMARIZED RATE DATA

Initial pressure, cm.	t_{25}, sec.	t_{50}, sec.	Initial pressure, cm.	t_{25}, sec.	t_{50}, sec.
Temperature, 170.2° C.					
3.02	410	940	0.64	535	1270
2.08	433	972	0.59	570	1300*
1.50	446	1045	0.44	660	1390
1.07	468	1060	0.33	660	1500*
0.75	525	1180*			
Temperature, 161.7° C.					
3.40	720	1710	1.00	1080	2520*
2.74	810	1930	0.97	1127	2600
2.20	880	1860	0.81	1155	2680*
1.98	920	2120	0.73	1162	2700*
1.93	960	2210	0.61	1176	2675
1.50	957	2380	0.59	1320	3000*
1.33	1094	2400	0.52	1425	3100
1.24	1065	2400	0.52	1283	3000*
1.18	1004	2400	0.38	1455	3220*
1.12	960	2500	0.37	1500	3300*
1.06	1053	2580	0.24	1800	3960*
1.04	1100	2500			
Temperature, 153.5° C.					
2.73	1885	4180	0.67	2900	— *
1.65	2176	4980	0.60	3460	— *
1.25	2210	5200	0.54	3000	—
1.00	2560	— *	0.37	3330	— *

NOTE.—*In runs marked *, a stopcock was used in the reaction system.*

TABLE III

EXTRAPOLATED VALUES OF RATE DATA

Temp., °C.	170.2	161.7	153.5	145.2
t_{25}, sec.	280	580	1420	3400
t_{50}, sec.	680	1470	3480	

Discussion

The falling-off in rate at low pressures in unimolecular decompositions may be described by the Kassel theory. Kassel assumes that reaction occurs when a molecule which possesses j quanta divided among s oscillators has m localized in one particular oscillator. The oscillators are considered to be identical and of frequency ν. The rate constant, k, at low pressures may then be expressed relative to the limiting high pressure rate, k_∞, by the relation

$$\frac{k}{k_\infty} = \left(1 - e^{-\frac{h\nu}{kT}}\right)^s \sum_{j=m}^{\infty} \frac{\binom{j-m+s-1}{j-m} e^{-\frac{(j-m)h\nu}{kT}}}{1 + \frac{A}{aN}\frac{j!\,(j-m+s-1)!}{(j-m)!\,(j+s-1)!}}$$

A is a measure of the rate of energy redistribution in the molecule, and is obtained empirically from the high pressure rate; a is the collision factor $4\sigma^2\left(\frac{\pi kT}{m}\right)^{\frac{1}{2}}$, where σ is the collision diameter.

In applying the relation, m must be so chosen that the value of the frequency (which is related to it by the expression $mh\nu = E/N_o$, where E is the energy of activation and N_o is Avogadro's number) is within the range of frequencies which are indicated by other data such as the Raman spectrum. The value of s is given by the relation $3(n - 2)$, where n is the number of atoms in the molecule.

Fig. 1 gives the theoretical curve for $s = 15$, $\sigma = 8 \times 10^{-8}$cm., and $m = 17$. The circles are experimental values.

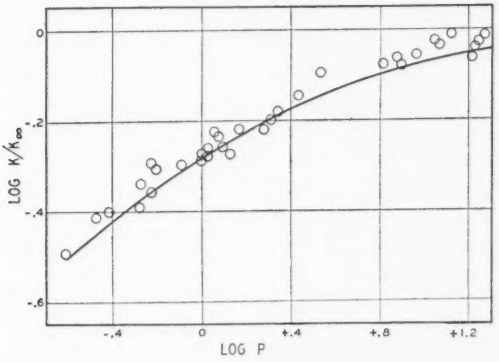

FIG. 1. *Falling-off in rate at low pressures. The circles are experimental points. The solid line is the theoretical curve for* $s = 15$, $\sigma = 8 \times 10^{-8}$ *cm.*, $\bar{\nu} = 779$ *cm.*$^{-1}$.

The value of $\bar{\nu}$ corresponding to the value chosen for m is 779 cm.$^{-1}$, a value consistent with the vibrational frequencies obtained from the Raman spectrum, *viz.* 420 to 1578 cm.$^{-1}$ (1).

The value of σ is not unreasonable but is slightly greater than the collision diameter to be expected for a molecule such as chloropicrin. However, the value for effective energy exchange with high energy molecules may well be somewhat different from the ordinary collision diameter. However, the extrapolation to obtain the high pressure rate is not very accurate, and it is possible that the true value of k_∞ may be greater by a small percentage than that used. If such is the case, the curve could be fitted to the data by employing a value of σ considerably smaller.

The value of s is of particular interest. Most molecules which undergo unimolecular decomposition contain C—H bonds, which possess such a high frequency that they are not thermally excited at decomposition temperatures. As a result the value of s is less than that given by the relation $s = 3(n - 2)$. Chloropicrin, however, contains no hydrogen atoms, and consequently should have all its oscillators thermally excited at the temperatures employed here. The fact that the theoretical value of s is satisfactory thus furnishes additional confirmation of the essential truth of unimolecular theory.

References

1. MILONE, M. Gazz. chim. ital. 63 : 453-456. 1933.
2. STEACIE, E. W. R. and SMITH, W. McF. J. Chem. Phys. 6 : 145-149. 1938.

ANALYTICAL NOTES. I.[1]

By C. W. Davis[2]

Abstract

An organic selenide is decomposed with an oxidizing mixture containing an excess of halogen. Selenium is determined gravimetrically as the metal.

The same oxidizing mixture is used for the decomposition of an organic mercury compound commonly used as a seed disinfectant.

A method is described by means of which elements difficult to separate may be determined by using two analytical methods followed by simple algebraic calculation for the unknowns.

Solid calcium acetate is used to retain the phosphorus on ignition of soybean oils.

Selenium in Organic Compounds

Selenium, like sulphur, forms dioxides and trioxides and unites with various metals to form compounds corresponding to the sulphides. Selenic acid closely resembles sulphuric acid. An important difference is the ease with which hydrochloric acid reduces the free acid and its salts to selenious acid. Sulphur dioxide will reduce selenium in the quadrivalent state to the metal. Early literature (1) contains many references to the difficulty of accurate determination of selenium and to the interference of nitric acid with the reduction.

A distillation apparatus with ground glass joints was used to study the decomposition of ethyl diselenide with an oxidizing mixture containing an excess of halogen. Nitro-chlorate mixture converted the selenium to a stable form such as selenic acid or selenates. The distillates after the addition of water and sulphuric acid and boiling off an equal volume of liquid contained no appreciable selenium. The traces of nitric acid remaining in the mixture containing sulphuric and selenic acids do not interfere with the quantitative reduction to selenium metal, provided that the selenic acid solution is added slowly to a large excess of hydrochloric acid saturated with sulphur dioxide as described by Lundell (4).

Examples

Ethyl diselenide. Calcd.: Se, 73.2%. Found: Se, 73.2%.

B.D.H. Sodium selenite. Calcd.: Se, 45.8%. Found: Se, 46.1%.

Mercury in Organic Compounds

Since mercury is completely volatilized when its compounds are ignited or fused with sodium carbonate, and since it is partly volatilized when solutions containing its salts are evaporated or boiled, the decomposition of organic mercury compounds without loss of mercury has presented some difficulties.

[1] *Manuscript received March 26, 1938.*
Contribution from the Division of Chemistry, National Research Laboratories, Ottawa, Canada.

[2] *Chemist, National Research Laboratories, Ottawa.*

Fitzgibbon (2) writes a brief survey of the well known procedures for determining mercury and recommends reduction with formaldehyde in the presence of gelatin, and titration iodometrically. This titration method was proved to be more accurate than two other methods, *viz.*, direct titration and reaction of mercuric sulphide with excess iodine. Fitzgibbon decomposes such compounds as ethyl mercuric chloride with bromine and sulphuric acid under reflux. This method of decomposition is slow because a large amount of reduced mercury rises above the acid during the procedure.

In the present work nitro-chlorate mixture was used in a narrow-necked 260 cc. Erlenmeyer flask. Decomposition was rapid, sometimes almost explosive, but on the whole the method was preferable to the slower one. Excess chlorine and nitric acid were eliminated by the addition of water and sulphuric acid and subsequent boiling until the volume was small. Several distillates were tested but no volatile mercuric chloride could be detected.

Example

Ethyl mercuric chloride. Calcd.: Hg, 75.67%. Found: Hg, 75.7, 75.5%.

Bromine and Chlorine in Organic Compounds

The quantitative separation of bromides from chlorides is difficult. According to Lundell (4), small amounts of chlorine can be separated from large amounts of bromine by oxidation with potassium bi-iodate. Separation can also be effected by oxidation with potassium permanganate and distillation, but the exact time at which all the bromine is distilled off is difficult to detect.

None of these methods proved satisfactory in an analysis of a sample of ethyl mercuric halide (prepared by means of the Grignard reagent). A simple yet accurate procedure for an unknown mixture is as follows.

Decomposition is effected by Robertson's (6) method. The halides in nitric acid solution are treated with excess silver nitrate in known amount and the excess is determined by Volhard's method. The weight of mixed silver bromide and chloride is ascertained. The amount of silver in the precipitate can be calculated from the normality and amount of silver nitrate solution that has reacted. Algebraic equations are solved in order to determine the percentages of bromine and chlorine. The method is simple and the results quite satisfactory. The general principle applied is analogous to that used in finding the approximate percentages of potassium and sodium in a mixture by calculation from the weight of their fused salts and chlorine content as determined by either Mohr's or Volhard's method. The determinations here are of interest in the analysis of commercial liquid soaps.

Example

(1) One gram of unknown yielded 0.6490 gm. of a mixture of silver bromide and silver chloride; this mixture contained 0.4014 gm. of silver. The weight of the bromine and chlorine in the mixed halides is therefore 0.2476 gm. (24.76%). If x = percentage bromine, and y = percentage chlorine, $x + y = 24.76$.

Then, $4.05x + 4.05y = 100.28$, and $2.35x + 4.05y = 64.90$, from which $x = 20.81\%$, $y = 3.95\%$.

(2) One gram of a mixed salt prepared from a soap contained 51.7% chlorine.

If x = percentage potassium chloride, and y = percentage sodium chloride, $x + y = 100$.

Then, $47.5x + 60.8y = 5170$, and $47.5x + 47.5y = 4750$, from which $x = 31.6\%$, $y = 68.4\%$.

Phosphorus in Soybean Products

The phosphorus in soybean oils is in the form of phosphatides (3) which are very readily coagulated. The decomposition of soybean oils by oxidizing acids is a laborious procedure and the large amount of reagents used interferes with the separation of phosphate.

Calcium acetate solution (5) has been used to retain the phosphorus on ignition of organic compounds such as casein. The ignition method in the present work was rapid, and it was found that the phosphorus was retained by the addition of 2 gm. of powdered calcium acetate to even 20 or 30 gm. of oil. This procedure allows the estimation of phosphorus by macro technique in oils containing very small amounts. The oil, covered with the calcium acetate in a porcelain crucible, is heated, ignited, and allowed to burn over a Bunsen flame. Ignition of residual carbon is effected in an electric muffle. The calcium phosphate and lime are dissolved in hydrochloric acid and water. Ferric chloride, in amount proportional to that of phosphate, is added to the solution. Ferric hydroxide and phosphate are precipitated with ammonia, and subsequent filtering eliminates most of the lime. The precipitate is dissolved in acid and phosphorus is determined by a standard molybdate procedure. Results can be checked by other methods of decomposition.

That this method gives good results with soybean oils is probably due to the nature of the phosphatide content. It is reasonable to believe that the addition of calcium acetate and the strong heating causes coagulation and intimate mixture of the phosphatides with calcium acetate as they settle to the bottom of the crucible.

References

1. Bradt, W. E. and Lyons, R. E. Proc. Indiana Acad Sci. 36 : 195-201. 1926.
2. Fitzgibbon, M. Analyst, 62 : 654-656. 1937.
3. Halliday, G. E. Oil & Soap, 14 : 103-104. 1937.
4. Hillebrand, W. F. and Lundell, G. E. F. Applied inorganic analysis. John Wiley and Sons, Inc., New York. 1929.
5. Shaw, R. H. Ind. Eng. Chem. 12 : 1168-1170. 1920.
6. Thorpe, J. F. and Whiteley, M. A. A student's manual of organic and chemical analysis, qualitative and quantitative. Longmans, Green and Company, Ltd., London. 1926.

THE HEAT CAPACITY AT CONSTANT VOLUME OF THE SYSTEM ETHYLENE NEAR THE CRITICAL TEMPERATURE AND PRESSURE[1]

BY D. B. PALL[2], J. W. BROUGHTON[3], AND O. MAASS[4]

Abstract

The heat capacity of ethylene at constant volume has been investigated through the critical range, between 6.5° and 27° C., at an average density slightly greater than the critical. The heat capacity in the immediate neighborhood of the critical temperature is found to be a function of the previous thermal treatment of the system. The results indicate the persistence of a large amount of molecular interaction in ethylene above the critical temperature, and are in agreement with the concept that the liquid state of aggregation can persist above the temperature at which the visible meniscus disappears.

Introduction

A large amount of evidence which seems to indicate that phenomena in the critical region are more complex than is indicated by the simple theory of Andrews (1) and Van der Waals has been accumulated. In particular, a series of reports from this laboratory have pointed to the persistence of the liquid state above the critical temperature, (7, 8, 9, 10). Most recently the work of Maass and Geddes (5), and of McIntosh and Maass (6), has confirmed the existence of a region in which the density of ethylene not only fails to follow the classical density-temperature parabola, but is also a function of the thermal history of the system.

These phenomena appeared to be explicable only in terms of molecular interaction. Any such molecular interaction must show up as a large effect in the heat capacity of the system, since every intermolecular bond represents an extra mode for heat absorption.

The apparatus designed to make these thermal measurements had to meet a number of exacting conditions. The pressures encountered in the critical region are high. Measurements must be made over very small temperature ranges. During the course of a run, the material should be as nearly as possible at temperature equilibrium; hence, the rate of heating must be slow.

Experimental

An adiabatic electrical calorimeter (Fig. 1) was used. A is a $\frac{1}{4}$ in. welded steel container, vacuum tight. F is a steel cylindrical bomb containing the material whose heat capacity is to be determined. The bomb is immersed in a mercury bath in the light steel container C. In the mercury, D, is a perforated steel cylinder E, on which is wound a copper heating element. The

[1] *Manuscript received June 7, 1938.*

Contribution from the Division of Physical Chemistry, McGill University, Montreal, Canada, with financial assistance from the National Research Council of Canada.

[2] *Graduate student, McGill University, and holder of a bursary, 1936–1937, under the National Research Council of Canada.*

[3] *Demonstrator, McGill University, at the time of the research.*

[4] *Macdonald Professor of Physical Chemistry, McGill University, Montreal, Canada.*

supports are of bakelite cut to a knife edge at the top. Attached to the walls are 12 radiation thermels, one of which is shown at *B*. These are copper-constantan thermocouples connected in series. The leads from the bomb heater to the outer electrical circuit pass through the tube shown. Another tube serves for outside connection to the thermocouples, and a third is used for evacuation.

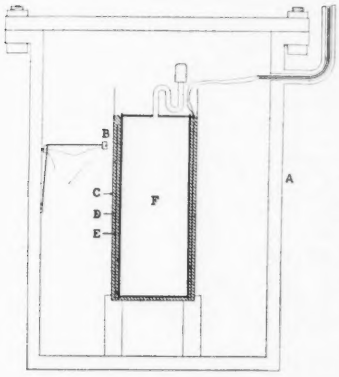

FIG. 1. *Diagram of the calorimeter.*

The outside electrical arrangements include a potentiometer which can be connected across either the bomb heating coil or a standard resistance in series with it. The thermocouples are connected directly in series with a low period, highly sensitive galvanometer, which shows a 1 cm. deflection for a 0.001° C. difference in temperature between the inner and outer parts of the calorimeter.

The calorimeter is immersed in a water bath fitted for very efficient stirring. A sensitive mercury-toluene thermoregulator made it possible to control the temperature within ±0.003° C. over long periods. The bath temperature could be controlled by hand to within less than 0.001° C.; thus heat losses in the calorimeter were quite negligible. Temperatures were measured by means of a Beckmann thermometer, which, when fitted with a special magnifying device, could with practice be read to within 0.0003° C. The absolute calibration, against a platinum resistance thermometer, was good to within 0.001°.

The bomb itself is illustrated in Fig. 2. It is constructed of welded steel, with 0.09 in. walls. The steel goose neck *D* was attached to the copper tube *C*, in which had been placed a piece of wire solder, at *E*. After the requisite amount of ethylene had been distilled in, the tube was heated at *A* to melt the solder, and pinched off at *B* after the seal had been made. The amount of ethylene distilled in was calculated to be 10.66 gm.; after a year during which the pressure in the bomb averaged 50 to 60 atm., it was weighed and opened, and the weight of ethylene was found to be 10.653 gm. It is seen, therefore, that the seal was air tight.

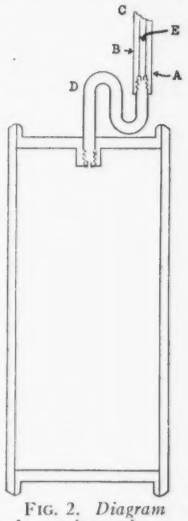

FIG. 2. *Diagram of container, showing method of sealing.*

The time during which current was passed through the heating coil was measured by means of a chronometer. This had been calibrated and was not appreciably in error. The potentiometer and standard cell had also been calibrated to 1 part in 10,000. The

ethylene was tank material supplied by the Ohio Chemical Company for anesthetic purposes; it was purified by low temperature distillation three times before using.

In the course of a run, the initial temperature of the bomb is determined by reading the outside temperature with no deflection in the thermel galvanometer. The heating coil is then turned on, the exact time being noted. Adiabatic conditions are maintained by raising the bath temperature simultaneously with that of the bomb, the reading of the thermel galvanometer being kept at zero. E.m.f. readings across both the heater and the standard resistance are noted at regular intervals, and the time when heating is stopped is recorded. Then, adiabatic conditions still being maintained, time is allowed for temperature equilibrium to be established in the bomb assembly, and the final temperature determined in the same way as the first. The rate of heating is about 1.5° per hr. The heat capacity is then calculated from the average value of the two e.m.f's, the heating time, and the temperature interval.

All other experimental errors were negligible compared with the error in determining temperature intervals. Although the Beckmann thermometer could be read to within 0.0003° C., it appears that owing to hysteresis effects its ultimate accuracy in measuring differences is about 1 part in 1000. This then is the accuracy of the determination of the heat capacity of the assembly—container, plus mercury, plus ethylene. When the measurements are made over very small ranges (less than 0.5° C.) this limit is of course increased.

A note should be added regarding "time lags". Outside of the range 8° to 9.5° C., temperature equilibrium after heating had been stopped was generally established in 10 min. Sometimes, however, the time required for equilibrium was much longer than this. It was considered to be of some interest to take the value of the changing temperature at intervals, until an asymptotic final value had been reached. These are included and systematized in the results under the heading "Time Lags".

Results

Heat Capacity Measurements

Values for the heat capacity of the system are given for the range 6.5° to 27° C. With the exception of the first three results in Section B of Table I, the measurements in the range 6.5° to 9.5° C. were made with two phases coexisting. The heat capacity of the system changes very rapidly in this region; consequently, it was necessary to make runs over very small temperature intervals. Furthermore, in the neighborhood of 8.5° to 9.5° C. long periods were required after heating for the establishment of equilibrium. Both these factors reduce the accuracy of the results obtained in this region compared with those in other temperature ranges.

TABLE I

HEAT CAPACITY AT CONSTANT VOLUME OF THE SYSTEM ETHYLENE BELOW THE CRITICAL TEMPERATURE. AVERAGE DENSITY = 0.2255

A Initial temperature approached from below 8° C.				*B* Initial temperature approached from above 15° C.	
Range, °C.	Av. heat capacity, cal./°C./gm.	Range, °C.	Av. heat capacity, cal./°C./gm.	Range, °C.	Av. heat capacity, cal./°C./gm.
9.39 – 9.59	0.622	8.75 – 8.96	1.418	9.38 – 9.54	0.633
9.36 – 9.50	0.694	8.66 – 8.86	1.349	9.37 – 9.57	0.647
9.26 – 9.46	0.918	8.66 – 8.86	1.359	9.36 – 9.50	0.663
9.17 – 9.37	1.184	8.41 – 8.61	1.320	9.29 – 9.52	0.651
9.06 – 9.25	1.405	8.21 – 8.41	1.269	9.26 – 9.48	0.705
8.96 – 9.16	1.305	8.03 – 8.21	1.255	9.16 – 9.36	1.082
8.86 – 9.06	1.430	7.47 – 7.96	1.251		
8.806 – 9.075	1.402	6.49 – 7.47	1.169		
8.80 – 8.99	1.320				

Density determinations have demonstrated that near the critical temperature this property is dependent on the thermal history of the systems (4, 6). By analogy the heat capacity might also be a function of previous heat treatment; this has been tested and found to be true. In Table II, the columns headed "Homogeneous" contain the results of those measurements made by bringing the temperature of the system down from at least 5° above the critical temperature. Similarly the heading "Heterogeneous" means that the bomb temperature was brought up from at least 1.5° below the critical temperature before the run was made. Although time lags do not directly affect these results, it may be noted that for the heterogeneous type of run starting at 9.36° C. it was necessary to maintain the temperature constant for at least 14 to 16 hr. before a run was started, in order to ensure that temperature equilibrium had been established.

The maximum difference in heat capacity, depending on thermal history, is seen to be 4.5% in the range 9.36° to 9.50° and 2.6% in the range 9.36° to 10.36°.

Table III shows heat capacities of the system at temperatures higher than 13.7° C., where the material is always homogeneous. The results of Tables I and II are plotted in Fig. 3, and those of Table III, showing a minimum in the curve, in Fig. 4.

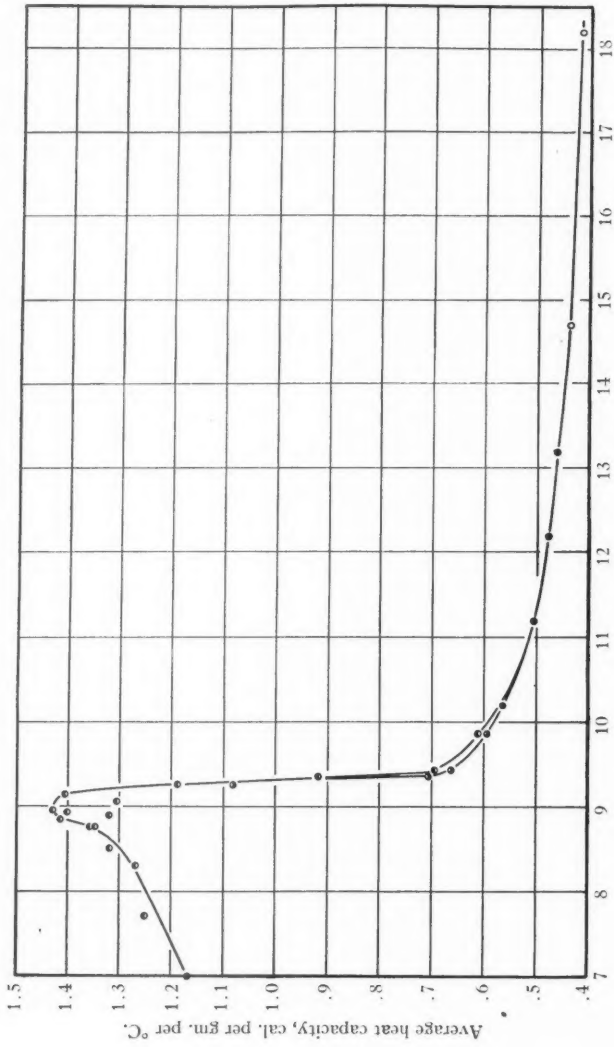

FIG. 3. *Heat capacity of ethylene, 7 to 18° C. Average density, 0.2255.* ●, *Temperature brought up from 8° or below before run started.* ◕, *Temperature brought down from above 15° before run started.*

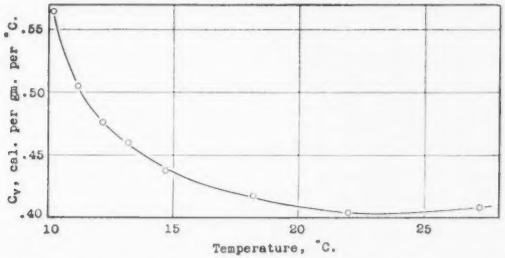

FIG. 4. *Specific heat of ethylene at constant volume, 10 to 27° C. Average density, 0.2255.*

TABLE II

HEAT CAPACITY OF ETHYLENE AT CONSTANT VOLUME
AVERAGE DENSITY = 0.2255

Temp. range, °C.	Heat capacity, bomb assembly, cal./°C.		Mean for bomb assembly		Absolute heat capacity, cal./°C./gm.		Difference, cal./°C./gm.
	Homogeneous	Heterogeneous	Homogeneous	Heterogeneous	Homogeneous	Heterogeneous	Heterogeneous minus homogeneous
9.36 – 9.50	40.72 40.99 40.69 40.90 41.05	41.36 41.07 41.35 41.07	40.87	41.20	0.663	0.694	0.031
9.36 – 10.36	40.18_5 40.18_8 40.11_9	40.29_0 40.37_7 40.26_3 40.37_5	40.15_1	40.32_6	0.594	0.609_5	0.015_5
9.7 – 10.7	39.88_8 39.79_3 39.86_6	39.85_4 39.97_7 39.87_6 39.83_4	39.85_3	39.87_9	0.563	0.565_5	0.002_5
10.7 – 11.7	39.29_4 39.22_3 39.29_7	39.31_9 39.24_7 39.30_8	39.27_1	39.29_1	0.504	0.505_5	0.0015
11.7 – 12.7	39.04_5 39.08_2 38.98_4	38.95_5 39.08_8 38.98_5	39.03_7	39.00_9	0.478	0.475_5	-0.002_8
12.7 – 13.7	38.88_8 38.91_6 38.89_3	38.84_5 38.91_4 38.87_3	38.89_9	38.87_3	0.461_5	0.459	-0.002_6
9.7 – 13.7	39.26_3* 39.25_9	39.26_5* 39.21_4					

* *Mean of 1° runs.*

TABLE III

SPECIFIC HEAT OF ETHYLENE AT CONSTANT VOLUME AT TEMPERATURES GREATER THAN 13.7° C.

Range, °C.	12.7 – 16.7	15.7 – 20.7	21.0 – 23.0	26.2 – 28.2
Heat capacity of bomb assembly, cal./°C.	38.70	38.61	38.51, 38.57	38.72, 38.60
Mean C_v, cal./°C./gm.	0.438	0.417_5	0.404_5	0.408

Time Lags

Geddes and Maass have shown that in the establishment of equilibrium in the critical-temperature–critical-pressure region there is a "time lag" depending on the previous thermal history of the system. In the calorimetric measurements described here a very large number of observations were recorded in establishing the time lag curves. However, a great simplification in presentation of data is possible, for the curves obtained on plotting temperature against time have the form of first order reaction plots. If the difference between the temperature at time t and the final asymptotic temperature is denoted by ΔT,

$$\frac{d(\Delta T)}{dt} = -k\Delta T$$

or in the integrated form,

$$\frac{\Delta T_0}{\Delta T} = kt \ ,$$

where ΔT_0 is the value of ΔT at zero time.

TABLE IV

TIME LAG

Material heated from 8.96 to 9.16 °C. in 560 sec. Zero time counted from instant at which heating is stopped. $\Delta T_0 = 31 \times 10^{-3}$ °C. $k = 3.4 \times 10^{-4}$ sec.$^{-1}$

Time, sec.	Temp., Beckmann	$\Delta T \times 10^3$ °C.	Time, sec.	Temp., Beckmann	$\Delta T \times 10^3$ °C.
610	1.3015	16.1	2560	1.2884	4.0
670	1.3002	14.8	2920	1.2879	3.5
720	1.2988	14.4	3190	1.2866	2.2
780	1.2988	14.4	3400	1.2862	1.8
940	1.2970	12.6	3760	1.2866	2.2
1000	1.2962	11.8	3940	1.2856	1.2
1060	1.2953	10.9	4480	1.2850	0.6
1210	1.2939	9.5	4680	1.2848	0.4
1370	1.2925	8.1	5340	1.2845	0.1
1600	1.2915	7.1	5860	1.2840	−0.4
1870	1.2898	5.4	6600	1.2845	0.1
1960	1.2897	5.3	7540	1.2843	−0.1
2320	1.2884	4.0	8440	1.2847	0.3

Thus, for each of the time lag curves a straight line is obtained when log ΔT is plotted against the time. A sample of the data recorded in establishing one of these time lags is given in Table IV, and the results are plotted with those of two other runs in Fig. 5. The slope of these lines is read as the value of k, the rate constant. The intercept on the zero time axis also has a meaning, since it represents the value of ΔT at zero time, and therefore corresponds to the total temperature drop. These are the ΔT_0 values; when multiplied by the total heat capacity of the bomb assembly they give the total amount of heat absorbed by the ethylene during the lag. For purposes of calculation, zero time is taken as half way through the heating interval. The k and ΔT_0 values are listed in Table V and plotted against the temperatures in Figs. 6 and 7.

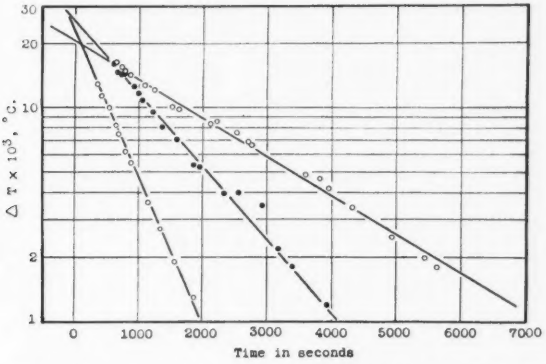

FIG. 5. *Sample time lags. Black circles correspond to Table IV.*

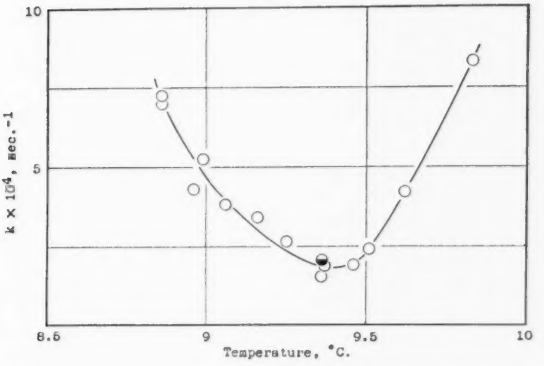

FIG. 6. *Rate constants for time lags.* ○, *Temperature brought up from below 8° C.* ◒, *Temperature brought down from above 14° C.*

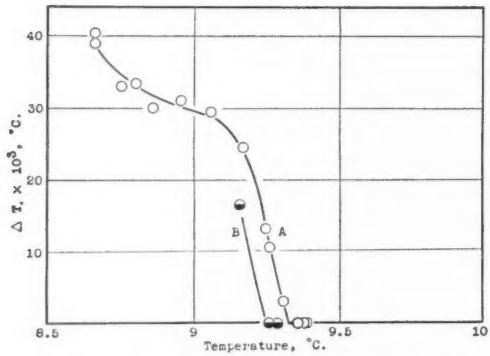

FIG. 7. ΔT_0 *for time lags.* ○, *Temperature brought up from below 8° C.* ◒, *Temperature, brought down from above 14° C.*

TABLE V

Range		Temp. interval, °C.	Time of heating, sec.	$\Delta T_0 \times 10^3$, °C.	$\Delta T_0 \times 10^3$, correct for a 0.2° interval	$k \times 10^4$ sec.$^{-1}$ $t_{1/2} = \frac{\log 2}{k}$
Initial temp. °C.	Final temp. °C.					
8.660	8.858	0.1981	560	38.5	39.0	7.27
8.664	8.855	0.1904	510	38.5	40.5	7.20
8.800	8.989	0.1892	505	31.5	33.5	5.36
8.746	8.856	0.2071	570	34.0	33.0	4.30
8.858	9.058	0.2005	555	30.0	30.0	3.81
8.957	9.163	0.2052	560	32.0	31.0	3.40
9.059	9.253	0.1942	525	28.5	29.5	2.68
*9.163	9.363	0.1977	520	16.5	16.5	2.06
9.170	9.367	0.1981	510	24.2	24.5	1.88
9.253	9.356	0.1030	260	13.0	13.0	1.51
9.260	9.461	0.2011	535	10.7	10.5	1.99
9.312	9.512	0.2000	400	3	3	2.4
9.16	9.834	0.67	180	70	—	8.3
9.16	9.622	0.46	165	35	—	4.2
*9.26	9.48	0.22	500	0	—	—
*9.29	9.52	0.23	500	0	—	—
*9.37	9.57	0.2	500	0	—	—
9.36	9.50	0.16	400	0	—	—
9.38	9.7	0.32	600	0	—	—
9.39	9.59	0.2	500	0	—	—

* *Initial temperature approached from above 15° C. All others approached from below 8° C.*

Discussion of Results

Pressure-volume-temperature Relations

It is essential to a thorough understanding of the results that a clear picture of the P-V-T relations be carried in mind. The average density chosen was 0.2255 gm. per cc. McIntosh and Maass (6) have investigated the system at this density with respect to dependence of density on thermal

history. The pressure also is accurately known to be a linear function of the temperature, and to be independent of the thermal history.

When the temperature of the system is raised at constant volume from 8° C. through the critical temperature (9.5° C.), its density does not become uniform throughout, but changes in a continuous manner, the two phases persisting up to about 12.5° C., although the meniscus vanishes at 9.5° C. Thus, when the temperature is raised from 8° through the critical temperature to 12.5° the density values follow Curve *A*, Fig. 8. There the density given is that of the lower phase. If now the temperature is lowered, the density values follow Curve *B*. Furthermore, liquid reappears now at 9.34° C., or 0.16° below the point at which the meniscus disappeared. On applying heat at any temperature represented by a point on *B* above 9.34°, the same course is followed. Evidently the system comprises two phases along *A* (for this reason it is referred to as heterogeneous); whereas along *B*, at temperatures greater than 9.34° C., the system is homogeneous.

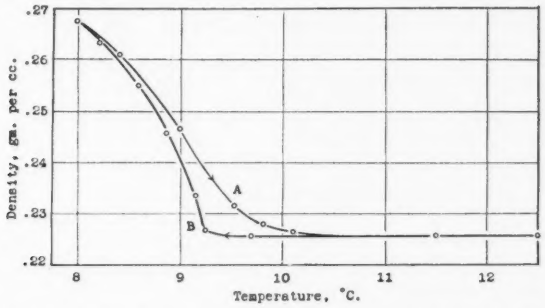

FIG. 8. *McIntosh and Maass isochore. Average density, 0.2255.*

Thermal History Effects

Consider two points on curves *A* and *B*, Fig. 8, at the same temperature, say 9.35° C. In Fig. 3, the point on the upper curve shows a heat capacity higher than that shown by the point on the lower curve. Suppose one assumes that these are equilibrium states, that is, that each of the systems would have the same properties after infinite time had elapsed, and furthermore that no attempt is made to distinguish any heterogeneity in the system, but it is considered as a whole—then their relative entropies can be discussed. One can bring the temperature of the system in the first state up to say 12.5° with absorption of Heat Q_1, then bring it back to the second state at 9.35° C., during which Heat Q_2 is removed. But Q_1 is greater than Q_2; hence, the system has undergone an increase in entropy.

Thus, on the assumption that the equilibrium state has been reached, it follows that it is possible to have in this region two systems with different entropies. It follows too that the system of greater entropy should be the

more stable. This is in accord with experiments which show that although the heterogeneous system can be changed to the homogeneous system without bringing the temperature of the system below the critical, the reverse change is not possible (4, 6).

An attempt can be made to form a kinetic picture of the system. In discussing the heterogeneous system, the phase of greater density will be referred to as the condensed phase, whereas the other will be termed the vapor phase. Evidently, the structure of the condensed phase must be more complex than that of the vapor phase; *i.e.*, there is more molecular interaction. This must correspond to an increase in the number of modes of taking up heat. Hence it would be expected that the heterogeneous system should have a greater heat capacity than the homogeneous system (see Table III).

For similar reasons it is not surprising that thermal history should appear as a factor in the time lag results (compare curves *A* and *B*, Fig. 7).

The Maximum in the Heat Capacity Curve

The occurrence of the maximum in heat capacity at 9° C. is readily explained. At temperatures below the critical, two phases are present. As the temperature is raised, liquid evaporates, and the heat of vaporization is measured together with the heat capacities of liquid and vapor, as well as any changes resulting from the compression of the vapor, or expansion of the liquid. Counteracting the effect of increased vaporization is the decreasing value of the heat of vaporization; furthermore, as the densities of liquid and vapor approach each other, a point will be reached at which the liquid will increase in mass as well as in volume, and evaporation no longer occurs. As the temperature is raised from say 7° C. the increasing evaporation predominates, but as the critical temperature is approached, the latter factors will predominate, and the heat capacity decreases.

The Minimum in the Heat Capacity Curve

At temperatures greater than 12.5° C. the system is always homogeneous. The specific heat continues to decrease up to about 22° C. Now, except in the critical region, C_v for ethylene shows an increase with temperature (3, 5). It can, moreover, be shown from the experimental value of $\left(\frac{d^2p}{dT^2}\right)_{v \text{ constant}}$ that this should hold at the pressures considered. This increase has been successfully explained in terms of increased absorption of heat by bond vibration at higher temperatures. Hence the decrease in heat capacity experimentally found cannot be explained by a molecular mechanism. Furthermore, no macroscopic changes take place. It follows therefore that heat must be absorbed as vibrational energy by bonds representing molecular interaction. There is therefore a large amount of intermolecular interaction in ethylene above the critical temperature, at these pressures, which does not entirely disappear until a temperature 13° C. above the critical has

been reached. At temperatures above this, a normal rise in specific heat with temperature is shown. These results are in qualitative agreement at least with those obtained by Callendar (2) for the specific heat of water. Exact comparison is not possible, since Callendar measured total heats at constant pressure.

Time Lags

It is more difficult to draw definite conclusions from the time lag data. The rate constant, k, is probably related to the value of $\frac{dp}{dv}$ and $\frac{d^2p}{dv^2}$ for the system. These approach zero at the critical temperature, at which it is seen that the rate constant shows a minimum (Fig. 6).

The ΔT_0 values correspond to the amount of "de-association" after heating through a 0.2° interval. These values are extraordinarily large. For instance, the absorption of heat for $\Delta T_0 = 0.030°$, $T_{initial} = 8.9°$ C., is $49.2 \times 0.030 = 1.48$ cal.; whereas during increase in temperature from 8.9° to 9.1° C., the ethylene itself absorbed $1.43 \times 10.66 \times 0.200 = 3.04$ cal.

Conclusions

It is possible to correlate very closely this work and density measurements. In neither is the classical result obtained when the system ethylene is brought through the critical temperature. Instead, the liquid state seems to persist after the meniscus has disappeared. This is shown in the one case by direct measurement of the density of the phases; in the other it is demonstrated by the difference in heat capacity of this two phase system and that of a homogeneous system, over the same range of temperature. In both, the difference in properties between the two systems becomes zero at about 10.5° C.

A large amount of molecular interaction exists in ethylene in the critical region. It must be concluded also that this is not confined to the condensed phase, but that the same is true of the vapor, but to a lesser degree. This follows from the decrease in heat capacity with temperature of the homogeneous system.

References

1. Andrews, T. J. Chem Soc. 23 : 74-95. 1870.
2. Callendar, H. L. Proc. Roy. Soc. A, 120 : 460-472. 1928.
3. Eucken, A. and Parts, A. Z. Physik. Chem. B, 20 : 184-194. 1933.
4. Heuse, W. Ann. Physik. 59 : 86-94. 1919.
5. Maass, O. and Geddes, A. L. Phil. Trans. Roy. Soc. A, 236 : 303-332. 1937.
6. McIntosh, R. L. and Maass, O. To be published.
7. Marsden, J. and Maass, O. Can. J. Research, B, 13 : 296-307. 1935.
8. Tapp, J. S., Steacie, E. W. R., and Maass, O. Can. J. Research, 9 : 217-239. 1933.
9. Winkler, C. A. and Maass, O. Can. J. Research, 9 : 65-79. 1933.
10. Winkler, C. A. and Maass, O. Can. J. Research, 9 : 613-629. 1933.

THE EFFECT OF MAGNESIUM-BASE SULPHITE-LIQUOR COMPOSITION ON THE RATE OF DELIGNIFICATION OF SPRUCE WOOD AND YIELD OF PULP[1]

By J. M. Calhoun[2], J. J. R. Cannon[3], F. H. Yorston[4], and O. Maass[5]

Abstract

The rate of delignification of resin extracted spruce wood-meal in magnesium base sulphite liquor has been determined at 130° C. over the concentration range 0.5 to 4% combined, and 2 to 10% free, sulphur dioxide. The rate of reaction is roughly proportional to the concentration of free sulphur dioxide when the combined is constant, but decreases with increase in the concentration of combined when the free is constant. The relation of the rate of delignification to the liquor composition cannot be expressed by any simple equation of the type:

$$\text{Rate of delignification} = K(\text{total } SO_2 - n \times \text{combined } SO_2),$$

where K and n are constants. The rate of cooking is somewhat greater in magnesium base sulphite liquor than in calcium base liquor of the same mole percentage composition.

The yield of pulp at any given lignin content is independent of the free sulphur dioxide over the whole concentration range, but increases with increase in the concentration of the combined to a maximum at about 3%, and decreases at slightly higher concentrations. When the concentration of combined sulphur dioxide is greater than 1% the yield of pulp obtained from magnesium base cooks is slightly higher than that from corresponding calcium base cooks.

Introduction

In an earlier paper (2) an investigation of the effect of calcium-base sulphite-liquor composition on the rate of delignification of spruce wood and yield of pulp was reported. It was found that the combined sulphur dioxide could be varied over only a comparatively small range of concentration without danger of precipitation of calcium sulphite during cooking. Therefore, the rate of delignification of spruce wood in magnesium base sulphite liquor was investigated, since the greater solubility of magnesium salts made possible a greater variation in the concentration of combined sulphur dioxide. It was hoped that this would permit a more precise correlation of the composition variables with the rate of delignification, and in addition prove an interesting comparison with the calcium system in regard to both the rate of cooking and the yield of pulp.

Sulphite liquors containing magnesia alone, or mixtures of lime and magnesia, have been used industrially to some extent. Hiller (3) states that higher yields and better quality of pulp have been obtained with magnesium base liquors, but no quantitative measurements of the rate of delignification have been made.

[1] *Manuscript received June 1, 1938.*

Contribution from the Division of Physical Chemistry, McGill University, Montreal, Canada. This investigation was carried out in co-operation with the Forest Products Laboratories of Canada, Montreal, and formed part of the research program of that institution.

[2] *Graduate student, McGill University, and holder of a bursary (1936–1937) and a studentship (1937–1938) under the National Research Council of Canada.*

[3] *Demonstrator, McGill University.*

[4] *Chemist, Forest Products Laboratories, Montreal, Department of Mines and Resources.*

[5] *Macdonald Professor of Physical Chemistry, McGill University, Montreal, Canada.*

Experimental

The experimental procedure followed was identical in every detail with that previously described for calcium base cooks (2), and the results in the two cases are, therefore, strictly comparable. Well seasoned, white spruce wood-meal (density, 0.43; mesh 40 to 100) was prepared from a single log and extracted with alcohol-benzene (1 : 2). All cooks were carried out in 100 cc. sealed Pyrex bomb tubes at 130° C. The liquor ratio (50 : 1) was sufficiently large to minimize any concentration changes during cooking. Six samples of wood-meal were cooked for different lengths of time in each liquor used. The mean liquor concentration for a given run was taken as the average of that for all the bombs, analysis being made after cooking. The pulp was filtered, washed, oven dried, weighed, and analyzed for lignin by the Ross-Potter method (5). All yields were calculated on the resin extracted, bone-dry wood basis.

The liquor concentration as determined at room temperature was corrected, in the manner previously described, for sulphur dioxide lost to the vapor phase at 130° C. The same correction as before was applied for the time required to heat the bombs to 130° C. This was calculated to be 0.22 hr., which was subtracted from the observed time that the bombs were in the bath.

Results and Discussion

The data for a typical run are given in Table I to illustrate the calculations. The lignin as percentage of the original wood was plotted on a logarithmic scale against the observed time of cooking for each run, *e.g.*, Series *B*, Fig. 1. The yield of pulp was also plotted against the observed time of cooking for each run, *e.g.*, Series *B*, Fig. 2. The uncorrected times to 80, 90 and 95% delignification were read from the lignin curve for each run, and the yields of pulp at the corresponding times were read from the yield curve. Because of the deviations of the reaction from the first order relation no attempt was made to calculate velocity constants. As in the case of the calcium base cooks, the reciprocal of the corrected time to 90% delignification was taken as the best measure of the rate.

TABLE I

DATA FROM A TYPICAL COOK (RUN NO. 83)*

Time in bath (uncorr.), hr.	Combined sulphur dioxide, %	Total sulphur dioxide (uncorr.), %	Total sulphur dioxide (corr.), %	Yield of pulp, %	Yield of non-lignin, %	Lignin, % of pulp	Lignin, % of original wood
0.75	0.97	7.99	7.93	77.3	61.5	20.4	15.8
1.50	0.94	7.86	7.72	65.7	57.3	12.8	8.4
2.25	0.93	7.76	7.70	57.1	53.6	6.04	3.45
2.75	0.91	7.82	7.79	54.1	52.6	2.76	1.49
3.25	0.91	7.84	7.76	52.3	51.0	1.94	1.01
4.00	0.88	7.79	7.67	50.5	50.0	1.01	0.51
Av.	0.92	7.84	7.76				

**See Table II for details.*

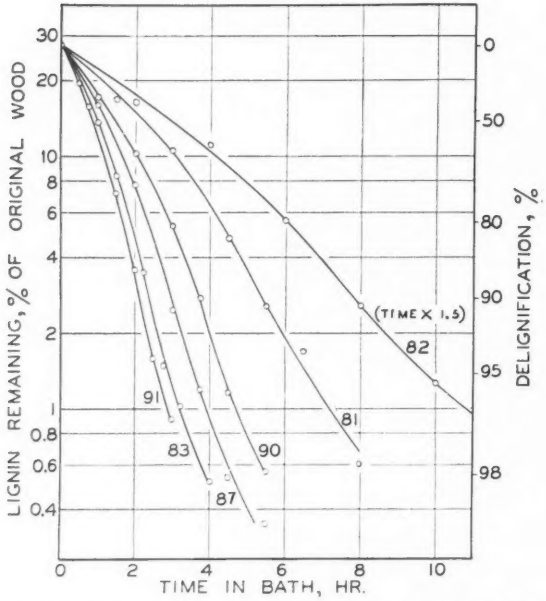

FIG. 1. *The effect of free sulphur dioxide concentration on the rate of delignification of spruce wood at 130° C. Series B. Magnesium base sulphite liquor; average combined sulphur dioxide 0.92%.*

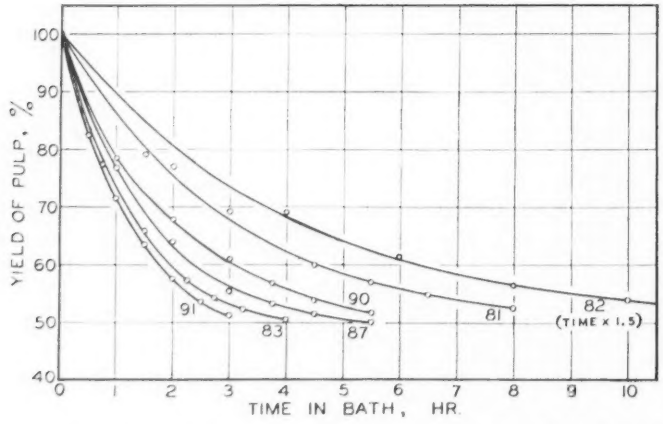

FIG. 2. *The effect of free sulphur dioxide concentration on the yield of pulp at 130° C. Series B. Magnesium base sulphite liquor; average combined sulphur dioxide 0.9%.*

TABLE II

SUMMARY OF THE EFFECT OF COMPOSITION OF MAGNESIUM BASE SULPHITE LIQUOR ON THE DELIGNIFICATION OF SPRUCE WOOD AT 130° C.

Run No.	Average final concentration of sulphur dioxide (corrected)			80% delignification		90% delignification		95% delignification		Time to 90% delignification (corrected), hr. $= t_{90\%}$	Rate of delignification $= 1/t_{90\%}$
	Combined, %	Total, %	Free (total − comb.), %	Time (uncorr.), hr.	Yield of pulp, %	Time (uncorr.), hr.	Yield of pulp, %	Time (uncorr.), hr.	Yield of pulp, %		
Series A											
105	0.40	2.15	1.75	6.40	54.3	8.28	50.3	10.25	48.0	8.06	0.124
104	0.39	3.40	3.01	3.82	54.0	4.83	50.3	5.98	47.8	4.61	0.217
102	0.45	4.70	4.25	2.70	56.8	3.53	52.7	4.32	50.2	3.31	0.302
103	0.44	6.51	6.07	2.05	57.0	2.63	52.4	3.26	50.2	2.41	0.415
107	0.45	8.63	8.18	1.57	55.3	2.00	51.0	2.45	48.4	1.78	0.562
Av.	0.43				55.5		51.3		48.9		
Series B											
82	0.88	2.44	1.56	9.13	61.0	11.78	56.6	14.60	54.0	11.56	0.086
81	0.98	3.95	2.97	4.25	60.8	5.38	57.0	6.65	54.2	5.16	0.194
90	0.92	5.01	4.09	2.96	60.8	3.75	56.7	4.34	54.3	3.53	0.283
87	0.91	6.16	5.25	2.37	60.2	3.02	55.6	3.60	53.5	2.80	0.357
83	0.92	7.76	6.84	1.89	60.6	2.40	56.3	2.88	53.5	2.18	0.458
91	0.92	9.05	8.13	1.70	60.8	2.12	56.3	2.62	52.9	1.90	0.527
Av.	0.92				60.7		56.4		53.7		
Series C											
96	1.93	4.62	2.69	6.45	63.8	8.60	59.0	10.75	56.2	8.38	0.119
92	1.92	5.64	3.72	3.85	64.7	4.83	60.6	5.86	57.8	4.61	0.217
98	1.97	7.03	5.06	2.74	62.7	3.47	58.2	4.15	55.8	3.25	0.308
84	1.90	8.59	6.69	2.00	65.5	2.56	60.6	3.15	56.5	2.34	0.427
94	1.94	10.36	8.42	1.67	64.3	2.08	59.3	2.41	56.7	1.86	0.538
Av.	1.93				64.2		59.5		56.6		

TABLE II—*Concluded*

SUMMARY OF THE EFFECT OF COMPOSITION OF MAGNESIUM BASE SULPHITE LIQUOR ON THE DELIGNIFICATION OF SPRUCE WOOD AT 130° C.—*Concluded*

Run No.	Average final concentration of sulphur dioxide (corrected)			80% delignification		90% delignification		95% delignification		Time to 90% delignification (corrected), hr. $= t_{90\%}$	Rate of delignification $= 1/t_{90\%}$
	Combined, %	Total, %	Free (total − comb.), %	Time (uncorr.), hr.	Yield of pulp, %	Time (uncorr.), hr.	Yield of pulp, %	Time (uncorr.), hr.	Yield of pulp, %		
Series D											
100	2.89	6.38	3.49	6.70	66.3	9.20	61.5	11.42	58.2	8.98	0.111
95	2.89	7.52	4.63	3.94	65.7	5.24	60.2	6.75	56.7	5.02	0.199
97	2.93	9.10	6.17	2.58	65.9	3.33	60.8	4.01	58.0	3.11	0.322
99	2.86	10.49	7.63	2.07	64.7	2.62	60.4	3.13	57.3	2.40	0.417
101	2.93	12.56	9.63	1.64	65.4	2.08	60.7	2.61	56.8	1.86	0.538
Av.	2.90				65.6		60.7		57.4		
Series E											
110	3.82	8.35	4.53	6.66	65.2	8.49	60.7	10.41	57.2	8.27	0.121
109	3.91	10.00	6.09	3.52	64.0	4.58	59.1	5.70	55.8	4.36	0.230
106	3.92	11.62	7.70	2.49	64.5	3.25	59.5	3.90	56.3	3.03	0.330
113	3.84	12.47	8.63	2.06	65.0	2.76	59.7	3.50	55.0	2.54	0.394
112	3.86	14.21	10.35	1.82	63.1	2.34	58.1	3.02	54.2	2.12	0.472
Av.	3.87				64.4		59.4		55.7		

A complete summary of the results of all runs is given in Table II. The range of concentration was from 0.5 to 4% combined, and 2 to 10% free sulphur dioxide.

The Relation of the Free Sulphur Dioxide to the Rate of Delignification

The average concentration of free sulphur dioxide (total − combined) for each run is listed in Table II, and is plotted against the rate of delignification ($1/t_{90\%}$) in Fig. 3. The dotted curve (C') is for Series C of the calcium base cooks taken from a previous paper (2) for comparison.

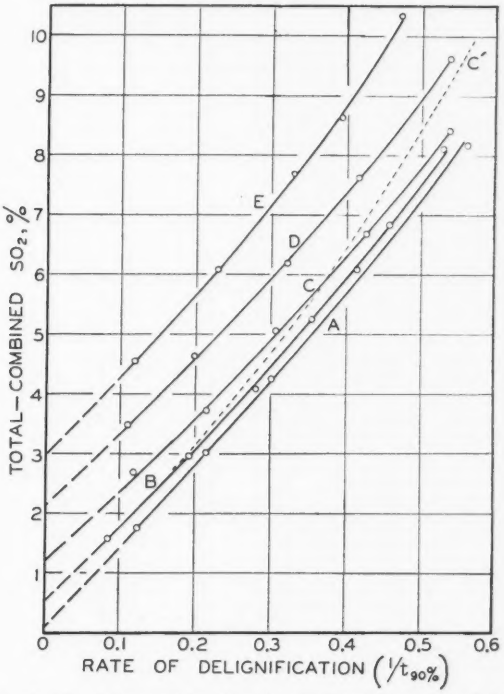

FIG. 3. *The relation of free sulphur dioxide concentration to rate of delignification of spruce wood at 130° C.* Mg *series A, B, C, D, E:—average combined sulphur dioxide, 0.43, 0.92, 1.93, 2.90, 3.78%, respectively.* Ca *series, C':—average combined sulphur dioxide, 0.90%.*

An inspection of Fig. 3 brings a number of interesting facts to light. It is observed that for magnesium base sulphite liquor the five series of combined sulphur dioxides give widely separated curves, none of which extrapolate to zero rate at zero concentration of free sulphur dioxide. Therefore, the rate of delignification of spruce wood in magnesium base sulphite liquor is decidedly not governed by the concentration of free sulphur dioxide alone, but decreases

with increasing concentration of the combined. This is contrary to the results obtained with calcium base cooks, which showed the rate of reaction to be virtually independent of the concentration of combined sulphur dioxide when the free is constant. This may possibly be due to inherent differences in the two liquors, but is more likely attributable to the fact that only a comparatively small variation in the concentration of combined sulphur dioxide is possible in the calcium base cooks because of solubility restrictions.

The rate of delignification in magnesium base sulphite liquor was also plotted for each series against the "total $-$ 1.5 $\times$ combined sulphur dioxide," and against the "total $-$ 2 $\times$ combined", as in the case of the calcium base cooks. The experimental data did not show any agreement with either relation. This can be made clearer in the following manner. The concentration of free sulphur dioxide for each series of combined, at the point corresponding to zero rate of delignification, was obtained by extrapolating the curves in Fig. 3. These values are listed in Table III, together with the total sulphur dioxide (free + combined), and the ratio of the total to the combined, all at zero rate of delignification.

Now, if the rate of delignification were related to the liquor composition in any simple manner such as,

$$1/t_{90\%} = K\,[\text{total } SO_2 - n \times \text{combined } SO_2]\ ,$$

where K and n are constants, then the ratio of the total to the combined sulphur dioxide at zero rate of delignification would also be constant and equal to n. If the rate of delignification were determined by the concentration of free or "excess" sulphur dioxide, n would equal 1.0, or 2.0, respectively. The last column of Table III shows that this is not so; n increases rapidly at first and then more slowly with increasing concentration of combined sulphur dioxide. Consequently, no relation of this type will fit the experimental results, and it would seem that the concentration of the active cooking agent in magnesium base sulphite liquor is not proportional to the analytical composition. Before any quantitative relation can be established, it will be necessary to obtain equilibria data on the magnesium system, which will enable the calculation of actual ion concentrations at cooking temperatures, as in the case of the calcium system.

TABLE III

THE COMPOSITION OF MAGNESIUM BASE SULPHITE LIQUOR AT POINTS CORRESPONDING TO ZERO RATE OF DELIGNIFICATION

Average combined SO_2, %	Free SO_2, %	Total SO_2, %	$\frac{\text{Total } SO_2}{\text{Combined } SO_2} = n$
0.43	0.10	0.53	1.23
0.92	0.45	1.37	1.49
1.93	1.20	3.13	1.62
2.90	2.10	5.00	1.73
3.87	2.95	6.82	1.76

The ratios of the total to the combined sulphur dioxide at zero rate of delignification listed in Table III suggest that no cooking would occur in

solutions of magnesium monosulphite containing no excess sulphur dioxide. This is probably not true, since Yorston (6) found that one-third of the lignin could be removed by cooking wood in neutral sodium sulphite solutions at 130° C. However, the rate of delignification, as determined by the time to reach 90% removal of lignin, may still be zero in magnesium sulphite solutions. Even if the curves in Fig. 3 did bend downward at low concentrations of free sulphur dioxide, it is only their relative positions with which we are concerned, and the statement made regarding the inadequacy of the above equation would still hold.

Consider, now, the absolute velocities of delignification in magnesium base sulphite liquor (Fig. 3, *B*), compared with that in calcium base liquor (Fig. 3, *C'*) of the same concentration of combined sulphur dioxide (0.9%). The reaction is noticeably more rapid in magnesium base liquor than in calcium base liquor of the same mole percentage composition. This agrees with the report of Berndt (1) who suggests that the magnesium salts of lignin sulphonic acids may be more soluble than the corresponding calcium salts.

Evidence has been presented (2) to show that the rate of delignification in calcium base sulphite liquor is determined by the product of the concentrations of the hydrogen and bisulphite ions. A comparison of the reaction rates in the two systems must, therefore, be made on the basis of the true ionic concentrations at the cooking temperature. Some preliminary results of King (4) show that the partial pressure of sulphur dioxide over magnesium base liquor differs considerably from that over calcium base liquor of the same mole percentage composition. Consequently, it is probable that the hydrogen and bisulphite ion concentrations in the two systems differ, and the higher reaction velocity in magnesium base liquor may not be due to any specific effect of the metal cation itself, but, rather to different equilibria conditions prevailing in the two liquors. As soon as the vapor pressure and conductivity data regarding the magnesium system are completed, it should be possible to settle these points.

From a practical point of view, the difference in the rate of pulping in magnesium and calcium base sulphite liquors is not great enough to be of any commercial importance. The great advantage of magnesium base liquor is that the danger of precipitation of sulphites, with consequent cooking difficulties and "liming-up" of digesters, is avoided.

The Relation of the Combined Sulphur Dioxide to the Rate of Delignification

To obtain a clearer picture of the effect of the combined sulphur dioxide on the rate of delignification of spruce wood-meal in magnesium base sulphite liquor, points were taken from the curves in Fig. 3 at constant concentrations of free sulphur dioxide, and replotted against the combined. The result is shown in Fig. 4, in which the dotted lines represent areas of extrapolation.

It is observed that a symmetric family of curves is obtained, corresponding to different concentrations of free sulphur dioxide. At low concentrations of combined and high free sulphur dioxide, the reaction rate does not vary

rapidly with the combined. However, at about 2% combined the curves all bend sharply in a direction which indicates a marked decrease in the rate of cooking with increase in the combined sulphur dioxide.

At the left side of Fig. 4 a line has been drawn through the points at which the concentrations of free and combined sulphur dioxide are equal, that is, where the composition of the liquors correspond to magnesium bisulphite containing no excess sulphurous acid. The position and slope of this line show that the rate of pulping in pure magnesium bisulphite solutions, although small, is appreciable and increases slowly with increasing concentration of magnesium bisulphite.

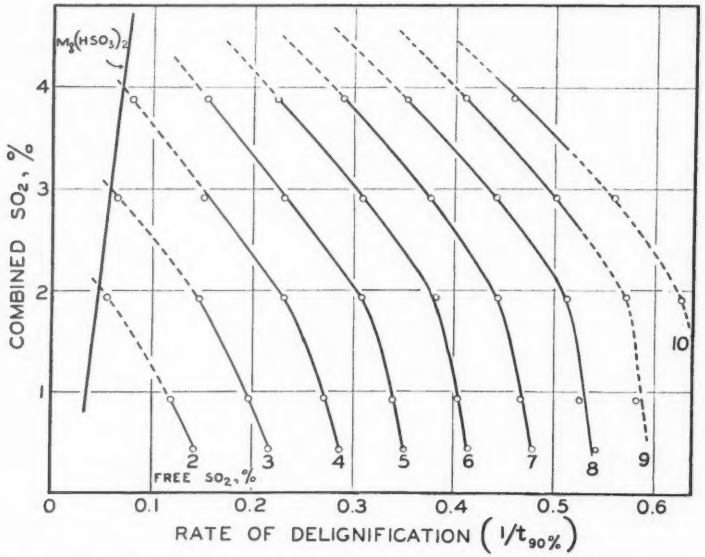

FIG. 4. *Rate of delignification of spruce wood in magnesium base sulphite liquor at 130° C. as a function of the combined sulphur dioxide concentration.*

The Effect of Liquor Composition on the Yield of Pulp

Table II shows that with magnesium base cooks the yield of pulp at a given lignin content is virtually independent of the concentration of free sulphur dioxide when the combined is constant, as was also found with calcium base cooks. In Fig. 5, the average yield of pulp for each series of combined, at 80, 90 and 95% delignification, is plotted against the average combined sulphur dioxide. The dotted curves show the same data for the calcium base cooks taken from a previous paper (2) for comparison.

It is observed that the yield of pulp from magnesium base cooks increases rapidly at first and then more slowly, reaching a maximum value at a concentration of about 3% combined sulphur dioxide, beyond which it drops slightly. Somewhat lower yields are obtained from magnesium than from calcium base cooks at low concentrations of combined sulphur dioxide, but higher yields are obtained at concentrations greater than 1% combined.

The effect of the liquor composition on the yield of pulp can be explained on the assumption that the rate of degradation of cellulose at a given temperature depends chiefly on the hydrogen ion concentration of the liquor. An increase in acidity or an increase in the length of the cook will result in a loss of yield. An increase in the concentration of combined sulphur dioxide at constant free, decreases the hydrogen ion concentration and hence increases the yield of pulp. At the same time, an increase in the concentration of combined sulphur dioxide at constant free also decreases the rate of delignification in magnesium base liquor; this lengthens the time required for cooking and so reduces the yield of pulp. These two opposing actions explain the maximum in the yield curves in Fig. 5. When the concentration of combined sulphur dioxide is constant, the rate of delignification is roughly proportional to the concentration of free sulphur dioxide. An increase in the free sulphur dioxide increases the hydrogen ion concentration of the liquor, but decreases the time required for lignin removal. This explains the approximate constancy of yield at different concentrations of free sulphur dioxide for a given concentration of combined.

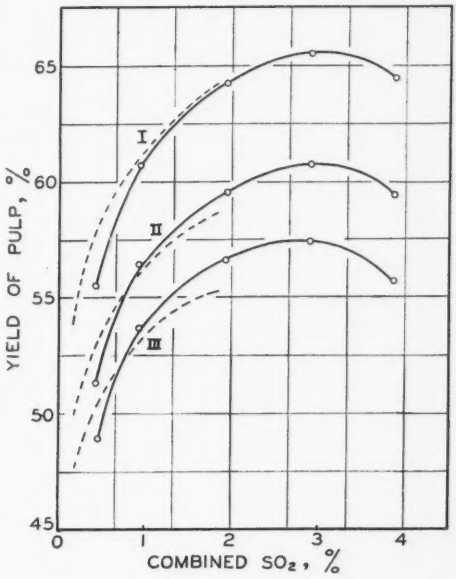

FIG. 5. *The effect of the combined sulphur dioxide concentration on the yield of pulp at 130° C. —— Magnesium base; -------- calcium base. Delignification I, 80; II, 90; III, 95%.*

The difference in the yields of pulp obtained from magnesium and calcium base liquor is not great enough to be of commercial interest. With either base, the yields of pulp in these experiments with liquors containing about 1% combined sulphur dioxide are considerably higher than those obtained in sulphite mills.

Conclusion

It is impossible at the present time to discuss the theoretical significance of the data presented here on the rate of delignification of spruce wood-meal in magnesium base sulphite liquor. A knowledge of the actual concentrations of the hydrogen and bisulphite ions for the liquor compositions and temperature used is required. At the time of writing, vapor pressure and conductivity measurements are being made on the system magnesium-oxide–sulphur-dioxide–water in this laboratory by King (4). When this information is available, an interpretation of the observed effect of the liquor composition on the reaction rate should be possible. It is hoped that the data obtained will assist in elucidating the mechanism of the delignification reaction. Particular interest is attached to the high concentrations of combined sulphur dioxide, which are not possible with a calcium base liquor.

From a practical point of view it should be noted that for cooking there would appear to be an optimum liquor composition of about 1.5% combined sulphur dioxide. At lower concentrations than this the yield of pulp shows a marked decrease, and at higher, the rate of delignification is abnormally low. The use of this concentration of combined sulphur dioxide with a calcium base liquor is not feasible.

References

1. BERNDT, K. Papier-Fabr. 24 : 561, 584. 1926.
2. CALHOUN, J. M., YORSTON, F. H., and MAASS, O. Can. J. Research, B, 15 : 457-474. 1937.
3. HILLER, O. Papier-Fabr. 31 : 195. 1928.
4. KING, T. E. Unpublished results, McGill University. 1938.
5. ROSS, J. H. and POTTER, J. C. Pulp and Paper Mag. Can. 29 : 569-571. 1930.
6. YORSTON, F. H. Forest Products Laboratories of Canada, Montreal. Project 70M. Progress Report No. 3. 1935.